Biogeochemical and omic evidence for paradoxical methane production via multiple co-occurring mechanisms in aquatic ecosystems

Authors

Elisabet Perez-Coronel[1,2*], J. Michael Beman[1]

[1]*Environmental Systems Graduate Group, and Sierra Nevada Research Institute, University of California Merced, Merced, USA.*

[2]*Ecology, Behavior and Evolution Section, University of California San Diego, La Jolla, USA.*

***Corresponding author:** Elisabet Perez-Coronel. University of California San Diego. 9500 Gilman Dr, La Jolla, CA, 92093 USA

e-mail for correspondence: elisabetperezcoronel@gmail.com

Phone: +12093558131

Abstract

Aquatic ecosystems are globally significant sources of the greenhouse gas methane (CH_4) to the atmosphere. However, CH_4 is produced 'paradoxically' in oxygenated water via poorly understood mechanisms, fundamentally limiting our understanding of overall CH_4 production. Here we resolve paradoxical CH_4 production mechanisms through CH_4 measurements, $\delta^{13}CH_4$ analyses, 16S rRNA sequencing, and metagenomics/metatranscriptomics applied to freshwater incubation experiments with multiple time points and treatments (addition of a methanogenesis inhibitor, dark, high-light). We captured significant paradoxical CH_4 production, as well as consistent metabolism of methylphosphonate by abundant bacteria—resembling observations from marine ecosystems. Metatranscriptomics and $\delta^{13}CH_4$ analyses applied to experimental treatments identified an additional CH_4 production mechanism associated with (bacterio)chlorophyll metabolism and photosynthesis by Cyanobacteria, and especially by Proteobacteria. Both mechanisms occured together within metagenome-assembled genomes, and appear widespread in freshwater. Our results indicate that multiple, co-occurring, and broadly-distributed bacterial groups and metabolic pathways produce CH_4 in aquatic ecosystems.

Introduction

Atmospheric concentrations of the potent greenhouse gas methane (CH_4) have increased significantly due to anthropogenic activity, representing an important component of climate change (1). However, these increases are superimposed on substantial spatial and temporal variability in natural sources of CH_4 to the atmosphere. Of all natural CH_4 sources, freshwater lakes are particularly important but poorly understood, with their estimated contribution ranging from 6 to 16% of all natural CH_4 emissions—despite accounting for only ~0.9% of the Earth's surface area (2). CH_4 emissions from lakes are conventionally viewed to be regulated by CH_4 production (occurring predominantly in anoxic sediments) and subsequent CH_4 oxidation in surface sediments and the water column (3). However, oversaturation of CH_4 has been consistently observed in oxygenated waters of aquatic systems (4). This observation indicates that CH_4 is produced under oxic conditions, and that the rate of CH_4 production exceeds CH_4 oxidation. Since archaeal methanogenesis is an obligate anaerobic process (5), oxic CH_4 production is typically referred to as the "methane paradox," and has been observed in oceans (6, 7), lakes (8, 9, 10), and aerobic wetland soils (11). Notably, paradoxical CH_4 production occurs near the surface, and so any produced CH_4 may readily flux to the atmosphere. Identifying which mechanisms produce CH_4 in oxygenated waters is therefore essential for our understanding of CH_4 fluxes and their contribution to climate change.

Although multiple mechanisms for paradoxical aerobic CH_4 production have been proposed, the degree to which these are active in freshwater lakes remains unknown. Initial studies suggested that CH_4 production under oxygenated conditions could be occurring in anoxic microsites in the water column—such as fecal pellets, detritus, and the gastrointestinal tracts of larger organisms such as fish or zooplankton (12, 13, 14). Several studies have also demonstrated a correlation between phytoplankton or primary production and CH_4 production (8, 9, 10). However, the underlying reason(s) for this relationship is unknown. One possibility is that methanogens reside on the surface of phytoplankton cells and produce CH_4 in presumably anoxic microsites (8). Bogard et al. (9) and Donis et al. (15) also hypothesized that several groups of methanogens have oxygen-tolerant or detoxifying pathways that could aid in CH_4 production in the presence of oxygen. For example, Angle et al. (11) characterized a methanogen candidate that possesses the enzymes to detoxify oxygen and produce CH_4 under aerobic conditions.

62 In contrast, the current prevailing view of marine ecosystems is that methylphosphonate
63 (MPn) is the main precursor of CH_4 production under oxic conditions—particularly in
64 phosphorus (P)-stressed ecosystems such as the open ocean (6, 16). MPn is the simplest form of
65 organic carbon (C)-P bonded compounds in aquatic ecosystems; microbial utilization of MPn,
66 and the consequent breakdown of the C-P bond, releases CH_4 as a by-product (6, 16, 17). A
67 broad range of marine and freshwater bacteria have the genomic potential to metabolize MPn
68 and produce CH_4, based on the presence of the multi-gene C-P lyase pathway in their
69 genomes. This includes multiple groups of Proteobacteria, Firmicutes, Bacteroidetes,
70 Chloroflexi, and Cyanobacteria (17, 18, 19). While expression of this pathway is thought to be
71 regulated by phosphate availability (17, 18, 19), the degree to which this occurs in freshwater
72 ecosystems is not well known (20, 21, 22). Finally, recent work indicates that cultures of marine
73 and freshwater Cyanobacteria can directly produce CH_4 (23). However, outside of a single
74 experiment (24), this has not been examined in aquatic ecosystems. More significantly, the exact
75 mechanism by which this occurs remains unknown. Given the widespread distribution of
76 cyanobacteria in the ocean and freshwater, identifying the potential mechanism(s) by which
77 cyanobacteria produce methane—and whether this capability may be present in other
78 photosynthetic organisms—is of broad relevance.
79 These proposed mechanisms for CH_4 production—(1) methanogenesis aided by
80 detoxifying genes or in anoxic microsites, (2) CH_4 production by breakdown of methylated
81 compounds, and (3) CH_4 production by Cyanobacteria—point to multiple mechanisms by which
82 CH_4 can be produced under oxygenated conditions. Many of these are recently discovered and
83 therefore poorly understood, and the degree to which they occur within different aquatic
84 ecosystems is largely unknown. We developed an experimental approach to disentangle these
85 mechanisms and determine which may produce CH_4 in freshwater lakes. We conducted
86 incubation experiments using surface waters from high-elevation lakes, in order to rule out
87 physical transport and focus on potential biological mechanisms of oxic CH_4 production. We
88 investigated specific mechanisms using a combination of CH_4 measurements over time,
89 experimental treatments and inhibitors, and 16S rRNA gene and transcript sequencing, while
90 also applying stable isotope analyses and metagenome and metatranscriptome sequencing to
91 selected experiments. Paradoxical CH_4 production was evident in multiple experiments and
92 experimental treatments, and could be attributed to MPn breakdown via widely-distributed

93 members of the *Comamonadaceae* family. However, experimental treatments, stable isotope
94 $\delta^{13}C$ signatures of CH_4, and metatranscriptomic data also point to a new potential mechanism of
95 aerobic CH_4 production carried out by photosynthetic bacteria.
96
97 **Results and Discussion**
98 Our experiments provide multiple lines of evidence for paradoxical CH_4 production in freshwater
99 lakes. Out of 19 total experiments conducted in five lakes in Yosemite National Park, 26% of
100 experiments showed unequivocal, monotonic CH_4 production in unamended controls; 16%
101 showed net oxidation in controls; 21% exhibited significant nonlinear patterns; and at least one
102 experimental treatment in 37% of experiments also showed significant production (see below;
103 based on replicate bottles incubated for at least 24 hours; Fig. 1). We observed the highest CH_4
104 production rates in Lukens Lake (e.g., L1 and L2 experiments), as well as consistent production
105 in Lower Gaylor Lake (LG1, LG3, and LG4) and Upper Cathedral Lake (UC1, UC2, UC3, and
106 UC4). Net CH_4 production rates ranged from 0.98 to 22.8 nM/h, with the majority of values <4
107 nM/h. These rates are consistent with the limited experiments previously conducted in other
108 freshwater lakes—e.g., 0.1-2.5 nM/h and 3.7 in Lake Stechlin, Germany (8 and 10
109 respectively)—and, on the higher end, our values are similar to the range reported by Bogard et
110 al. (9) for experimental manipulations in Lac Cromwell (2.08-8.33 nM/h). CH_4 turnover rates
111 also ranged from 5 to 146 days (with in situ concentrations ranging from 309-2839 nM),
112 consistent with turnover rates of ~18 days in Lake Stechlin (CH_4 concentration ~430 nM; 8),
113 ~2.2 days in Lac Cromwell (CH_4 concentration ~200 nM; 9), and 67 days in Yellowstone Lake
114 (CH_4 concentration of 46.3 nM; 21). Given these consistencies with observed rates in other
115 lakes, paradoxical CH_4 production rates in Yosemite appear broadly relevant.
116 Eleven experiments did not show monotonic increases or decreases, which could reflect
117 either (i) a complete absence of CH_4 metabolism at the time of sampling, or, more likely, (ii)
118 variations in the balance between co-occurring CH_4 production and consumption over time. For
119 example, initial CH_4 production could be followed by oxidation once CH_4 concentrations reach a
120 certain threshold required for oxidation (8). Conversely, initial decreases due to oxidation may
121 be followed by eventual production—for example through the development of P limitation that
122 triggers CH_4 production via MPn metabolism (6).We tested for nonlinear patterns using
123 ANOVA, and found two cases of initial CH_4 production followed by oxidation (LG1 and UC3;

124 Figure S1 and SI Text). It is also possible that production and oxidation proceed at similar rates,
125 leading to no net change in concentrations, even though CH_4 is actively cycled. In this case,
126 molecular data are useful for providing insight into the underlying dynamics. We consequently
127 examined expression of the particulate methane monooxygenase gene *(pmoA)* in
128 metatranscriptomes, and found that *pmoA* was expressed in the majority of the incubations
129 surveyed (SI Text).
130 Observed decreases in CH_4 concentrations, as well as omic data, are indicative of active
131 CH_4 oxidation that may obscure paradoxical production. Put another way, CH_4 is clearly
132 produced in incubations showing initial increases (UC3, LG1) or significant net increases (L1,
133 L2, LG3, LG4 and UC1); however, it may also actively occur in experiments showing no
134 significant change (or even consumption) over time, if CH_4 oxidation rates are equal to or greater
135 than production rates. We therefore evaluated potential paradoxical CH_4 production mechanisms
136 across experiments using multiple experimental treatments (BES, dark, high-light), and applied
137 16S rRNA sequencing, metagenomics, metatranscriptomics, and $\delta^{13}C$ stable isotopic analyses to
138 samples collected during these experiments.
139
140 *Methanogenesis*
141 We used these multiple approaches to test for phytoplankton- or particle-based methanogenesis,
142 as initial observations in freshwater lakes showed methanogens attached to phytoplankton (8),
143 while other work has suggested CH_4 production can occur in anoxic microsites on particles (12,
144 13, 14). In all experiments from 2017 and 2018, we included a treatment that consisted of the
145 addition of the methanogenesis inhibitor BES (2-bromoethanesulphonate). While there are some
146 caveats with its use (25), BES is widely used, including earlier tests of the CH_4 paradox (8, 10).
147 In our experiments, BES had an inhibitory effect on CH_4 production in four experiments, but
148 actually significantly increased CH_4 production rates in four experiments (see below), and had no
149 significant effect in the five remaining experiments (Fig. S2). In parallel, 16S rRNA sequencing
150 of DNA from experiments L1-6 and LG1-4 recovered no methanogen 16S sequences (out of 5.4
151 million total sequences; Table 1). Sequencing of 16S rRNA transcripts in RNA samples from
152 experiments L5-6, LG5-6, and UC3-4 recovered methanogen sequences in only two samples
153 (dark treatments from L5 and LG5), and total numbers were only 0.014% and 0.008% of all 16S
154 rRNA sequences (Table 1). Analysis of metatranscriptomes likewise showed that methyl

155 coenzyme A (*mcrA*; responsible for methanogenesis) transcripts were absent in LG6 and UC4(tf)
156 incubations and present at low levels in LG5, L7 and UC4(t0) (Fig. 2a). *mcrA* genes were absent
157 in all metagenomes, with the sole exception of the L6(tf) incubation (Fig. 2b). (Incubations were
158 monitored to confirm that they were under oxic conditions at all times.) Collectively these data
159 provide limited evidence—but not the complete absence of evidence—for water column-based
160 methanogenesis as source of CH_4, as BES reduced production in four experiments (Fig. S2),
161 methanogens were almost entirely absent and inactive based on 16S data (Table 1), and *mcrA*
162 transcripts and genes were rarely expressed and detected in metatranscriptomes and
163 metagenomes (Fig. 2).
164
165 *Methylphosphonate metabolism as a source of methane*
166 Instead, analysis of metatranscriptomes and metagenomes showed potential for CH_4 production
167 mechanisms other than conventional methanogenesis. In particular, we found evidence for
168 microbial metabolism of MPn based on the universal expression of alpha-D-ribose 1-
169 methylphosphonate 5-phosphate C-P lyase (*phnJ*) transcripts in metatranscriptomes (Fig. 2a).
170 *phnJ* is responsible for the cleavage of the C-P bond that results in CH_4 production from MPn;
171 this mechanism is thought to be the dominant paradoxical CH_4 production mechanism in the
172 ocean (16), but has been documented in only a limited number of freshwater lakes (20, 21, 22).
173 In addition to *phnJ*, phosphonate-binding periplasmic protein (*phnD)* genes (involved in the
174 binding component of phosphonate uptake; 26) were also universally expressed (Fig. 2). *phnJ*
175 and *phnD* genes were also recovered in all metagenomes (Fig. 2b).
176 The majority of *phnJ* and *phnD* genes were present in organisms of the same genera as
177 the metatranscriptomes, and over 40 different bacterial genera expressed or possessed *phnJ*
178 genes. This indicates that P assimilation from MPn is broadly distributed among surface water
179 microbes in these lakes. However, *phnJ* transcripts and genes were predominantly found
180 among organisms in the betaproteobacterial *Comamonadaceae* family: multiple
181 *Comamonadaceae* genera accounted for 20.9% of *phnJ* transcripts in metatranscriptomes and
182 27.4% of *phnJ* genes in metagenomes (Table S1). *phnJ* transcripts and genes from
183 *Sphingobacteriales* were also abundant in several samples (LG5 and LG6 metatranscriptomes,
184 L6 metagenomes). *Comamonadaceae* transcripts and genes showed notably high identity to
185 database sequences, with the majority of sequences showing >92% and up to 100% amino acid

186 identity to *Acidovorax, Hydrogenophaga*, *Limnohabitans, Polaromonas*, *Rhodoferax*, and
187 *Variovorax phnJ* sequences (Table S1).
188 16S data are consistent with this and demonstrate that *Comamonadaceae* were
189 universally present and abundant across experiments. In 16S rRNA gene sequence libraries from
190 experiments L1-6, LG1-4, and UC1, *Comamonadaceae* ranged from 2.04% (L6) to 11.6% (UC1)
191 of all sequences (Table 1), and were abundant in several incubations with significant CH_4
192 production (L1, L2, UC1). Sequencing of 16S rRNA transcripts in RNA samples from
193 experiments L5-6, LG5-6, and UC3-4 showed similar values (Table 1), and *Comamonadaceae*
194 reached 15% of all 16S rRNA transcripts in the UC3 and UC4 experiments (where CH_4 was
195 significantly produced in some treatments). Similar to *phnJ* results, 16S sequences from the
196 dominant *Comamonadaceae* ASVs showed high (98.8-100%) nucleotide sequence identity to
197 16S rRNA genes in sequenced genomes (Table S2).
198 Finally, we assembled and annotated metatranscriptomes and metagenomes to examine
199 whether particular groups possess and express multiple *phn* and related genes in parallel, as the
200 genes involved in phosphonate acquisition and utilization often cluster in genomes (18). We
201 found that *phnJ* genes commonly clustered with other *phn* genes on the same contigs,
202 particularly those from the *Comamonadaceae* (Table S3). For example, contigs >50 kb
203 containing *phnC*, *phnD*, *phnE*, *phnI*, *phnJ*, *phnK*, *phnL*, *phnM* were present in metagenomes
204 from the LG2 and L6 incubations, and were affiliated with the abundant freshwater bacterial
205 group *Limnohabitans* (31, 32, 33), as well as other members of the *Comamonadaceae,* such as
206 *Hydrogenophaga* and *Acidovorax.* Several longer contigs also contained *pst* or *pho* genes
207 involved in P uptake and metabolism (Table S3). P limitation is common in freshwater lakes, as
208 it is in the open ocean (34, 35, 36). High-elevation lakes in the Sierra Nevada are typically
209 oligotrophic (35, 37), and inorganic phosphate concentrations in the lakes sampled here are
210 consistently near the limits of detection (100 nM) by colorimetric techniques, with the vast
211 majority of measurements <200 nM (38, 39). Under these conditions, organic P compounds—
212 including phosphonates—could serve as important sources of P. Our findings are consistent with
213 this idea, and the presence and expression of *phnJ* genes indicates that several microbial groups
214 are capable of releasing CH_4 through the cleavage of the C-P bond in MPn (Fig. 2). Our data in
215 particular implicate multiple genera within the *Comamonadaceae* in MPn metabolism, given
216 high *phnJ* and 16S identities (Tables S1 and S2), recovery of contigs containing *phn* and other

217 genes involved in P acquisition and metabolism (Table S3), and their widespread presence and
218 abundance in all experiments (Table 1).
219
220 *Evidence for methane production by photosynthetic bacteria*
221 In addition to microbial use of MPn, Cyanobacterial photosynthesis was recently identified as a
222 possible source of paradoxical CH_4 production—yet the pathway by which Cyanobacteria
223 ultimately produce CH_4 remains unknown (23). Based on 16S rRNA genes and transcripts, and
224 metagenomes and metatranscriptomes, Cyanobacteria were common in our samples (Table
225 1). We used two additional treatments to partition the relative effects of CH_4 production vs.
226 oxidation and evaluate Cyanobacteria as a potential source of CH_4. First, we conducted light
227 versus dark treatments in some experiments, as (i) light has been shown to inhibit CH_4 oxidation
228 (40, 41, 42), and (ii) CH_4 production in cyanobacterial cultures was positively correlated with
229 light (23). As a result, dark treatments would be expected to have higher CH_4 oxidation rates,
230 lower cyanobacterial CH_4 production, and therefore lower CH_4 concentrations compared with
231 controls. Additionally, we increased light intensity in four experiments, which may have a two-
232 fold effect: (i) greater inhibition of CH_4 oxidation, and (ii) increased rates of CH_4 production
233 from Cyanobacteria or other phytoplankton (8, 9, 23). For both of these reasons, we expected to
234 observe higher CH_4 production rates under higher light levels.
235 Dark bottles showed mixed results, with four cases of CH_4 consumption (L4, LC1, and
236 LG6 at 24 hours and LG5 at 86 hours; all $p<0.05$), production in two cases (UC2 at 24 hours and
237 L5 at 74 hours; both $p<0.05$), and no significant difference in four experiments (L3, L7, LG4 and
238 UC3). In two of four experiments with high light treatments, we observed increased CH_4
239 production (L2 and UC4; both $p<0.05$). The UC4 experiment was particularly illuminating, as
240 higher light intensity significantly boosted CH_4 production rates by 62-fold compared with the
241 control (up to 3.2 nM/h; $p<0.0005$). This was among the strongest treatment effects observed
242 across all experiments (Fig. S2). BES also increased CH_4 production rate by 49-fold compared
243 with control in the UC4 experiment (up to 2.5 nM/h; $p<0.0005$, Fig. S2). This counterintuitive
244 effect suggests another source of CH_4.
245 To examine these responses in greater detail, we analyzed both the $\delta^{13}C$ stable isotope
246 composition of CH_4 produced during the UC4 experiment, as well as changes in gene expression
247 in response to experimental treatments in metatranscriptomes. We also directly compared these

248 results with the LG6 and L7 experiments, which did not show CH_4 production in BES or high-
249 light treatments. Consistent with a lack of significant CH_4 production in these experiments,
250 $\delta^{13}CH_4$ from multiple sampling time points showed no significant variation between treatments
251 in the LG6 and L7 experiments (Fig. 3a).
252 UC4 experimental data presented a clear contrast, as $\delta^{13}CH_4$ values were significantly
253 lower in the BES and high light treatments compared with controls (Fig. 3a). Along with
254 increased CH_4 concentrations (Fig. 3b), these data are indicative of an isotopically-depleted CH_4
255 source in the BES and high light treatments, which we calculate to be -56.9‰ to -57.0‰ based
256 on isotopic mass balance. These depleted values are substantially lower than atmospheric CH_4
257 samples collected at the same time (-45.2 to -47.4‰), and reflect isotopic fractionation by the
258 process producing CH_4 (43). Methanogenesis does lead to strong fractionation, and our
259 measured values fall at the upper end of typical $\delta^{13}CH_4$ values for methanogenesis (-110 to -
260 50‰; 43). However, *mcrA* expression declined to undetectable levels (Fig. 2) in these
261 treatments—which include BES, a methanogenesis inhibitor—suggesting another source. Strong
262 isotopic fractionation from MPn is unlikely, as the mean isotopic fractionation for CH_4 derived
263 from MPn is only 1.3‰ (44). MPn could be allochthonous (terrestrial) or autochthonous (based
264 on *pepM* results; Fig. 2), but in either case, is unlikely to be sufficiently ^{13}C-depleted to produce
265 the measured values. For example, the $\delta^{13}C$ value of organic matter in surface waters of nearby
266 Swamp Lake reaches a minimum of -37‰ (45). *phnJ* was also downregulated in both the BES
267 and high-light treatments (Fig. 4), further suggesting that MPn breakdown is not a major source
268 of CH_4 in these treatments. However, our isotopic data and metatranscriptomic data are
269 consistent with limited information available regarding photosynthetic CH_4 production, which
270 indicates that this is an isotopically light source (-55 to -45‰; ref. 23, 46).
271 Although the pathway by which Cyanobacteria produce CH_4 remains unidentified, Bižić
272 et al. (23) hypothesized that CH_4 is produced during photosynthesis owing to positive correlation
273 between light and CH_4. We used metatranscriptomic data to identify specific functions related to
274 photosynthesis that were significantly different in the treatments vs. the control, and that may
275 explain differences in CH_4 concentrations and isotopic composition. This is an advantage of
276 'omic data, as it is possible to examine previously unidentified potential mechanisms for CH_4
277 production. Through comparison of all functions across metatranscriptomes from the UC4
278 experiment, we identified two functions related to chlorophyll biosynthesis that were upregulated

279 and could potentially explain the increases in CH_4: ferredoxin:protochlorophyllide reductase
280 (DPOR) and chlorophyllide a reductase (COR) are involved in porphyrin and chlorophyll
281 metabolism, and both were significantly different between the control and the BES ($p<0.0005$)
282 and HL ($p<0.005$) treatments (Fig. 4). While not directly involved in photosynthesis, DPOR is
283 found in photosynthetic bacteria, Cyanobacteria, and green algae, and is involved in the light-
284 independent reduction of protochlorophyllide (47, 48). COR catalyzes the first step in the
285 conversion of chlorin to a bacteriochlorin ring during bacteriochlorophyll biosynthesis (49, 50,
286 51). Notably, both DPOR and COR are nitrogenase-like enzymes, and both were abundant in all
287 metatranscriptomes and metagenomes (Fig. 5). DPOR was found in several cyanobacterial
288 groups—such as *Pseudanabaena*, *Dolichospermum*, *Snowella* and *Oscillatoria*—in the
289 metatranscriptome data (Table S1). However, both DPOR and COR were particularly common
290 within the *Limnohabitans* and *Polynucleobacter* genera (36.3-54.5% of DPOR and COR
291 transcripts; Table S1), as some strains of these abundant freshwater bacteria are capable of
292 aerobic anoxygenic photosynthesis (33,52).
293 To further verify these findings, we mapped reads from the UC4 experiment, as well the
294 LG6 and L7 experiments (which did not show CH_4 production), to metagenome assembled
295 genomes (MAGs). MAGs were assembled as part of the Genomes from Earth's Microbiomes
296 (GEM) catalog (53), with 27 MAGs recovered from two Yosemite metagenomes. Five of these
297 MAGs were betaproteobacterial, including one *Rubrivivax* MAG, one *Polynucleobacter* MAG,
298 and three *Limnohabitans* MAGs. All five of these betaproteobacterial MAGs contained genes
299 for photosynthesis, including COR (Table S4). Three of these MAGs contained both COR and
300 DPOR, as well as multiple genes involved in phosphonate metabolism. Of the remaining two
301 MAGs, one lacked DPOR while the other lacked *phn* genes (Table S4), but these MAGs were
302 estimated to be 55-58% complete.
303 Based on read mapping to these MAGs, we examined patterns in transcripts that showed
304 differences in the BES and high light treatments of the UC4 experiment compared with the
305 control. We also examined differences between the UC4 experiment versus the LG6 and L7
306 experiments. We found that multiple photosynthesis genes from *Limnohabitans* MAG 5 were
307 highly expressed in UC4, while not detected at all in the LG6 and L7 experiments (Fig. 5c).
308 Furthermore, of >12000 genes present in the five MAGs, several of these genes showed the
309 highest overall number of mapped reads in the UC4 BES and high light treatments. Principal

310 among these were two subunits of COR, as well as associated photosynthetic reaction center
311 genes located on the same MAG scaffold (Fig. 5c). The *Limnohabitans* MAG 5 DPOR gene was
312 also highly expressed. In contrast, phosphonate metabolism genes were expressed at lower
313 levels and in similar levels in all metatranscriptomes.

314 DPOR and COR were expressed and present in all metatranscriptomes and metagenomes,
315 yet the overall expression of DPOR and COR was an order of magnitude higher in the UC4
316 experiment compared with the LG6 and L7 experiments (Fig. 5a). Differences in the expression
317 of DPOR and COR from *Limnohabitans* MAG 5 were even more pronounced. These patterns
318 are highly consistent with the lack of a $\delta^{13}CH_4$ isotopic signal in the LG6 and L7 experiments
319 compared with the UC4 experiment (Fig. 3). Based on the positive effects of BES and of high-
320 light on CH_4 production observed in the UC4 experiments, this mechanism may also be active in
321 the L2, L3, LG4, and UC3 experiments, where BES and high light also significantly increased
322 CH_4 production (Fig. S2). Decreases in CH_4 in dark treatments in several experiments may also
323 reflect decreased photosynthesis (alongside increased CH_4 oxidation; Fig. S2). Experimental data
324 also indicate that this mechanism is environmentally variable, given clear differences between
325 experiments (Figs. 3 and 5). However, these variations are consistent with the fact that
326 photosynthesis by *Limnohabitans* is variable, as photosynthesis is used to supplement
327 heterotrophy (52).

328 Based on these findings, we propose two potential mechanisms that could be involved in
329 paradoxical CH_4 production in oxic surface waters of freshwater lakes: (1) CH_4 may be produced
330 from methoxyl groups present in (bacterio)chlorophyll precursors, or (2) CH_4 production may be
331 catalyzed by DPOR and COR enzymes. In terrestrial plants, CH_4 is thought to be produced
332 aerobically from structural components—such as pectin, lignin and cellulose (54, 55, 56)—
333 mainly in plants under stress (such as increased temperature, UV radiation or physical damage;
334 57). Protochlorophyllide, chlorophyllide, and other bacteriochlorophyll precursors contain
335 methoxyl groups that have been shown to serve as precursors of CH_4 in plants (58), and a similar
336 mechanism may be active in Cyanobacteria and/or Proteobacteria under stress (presumably due
337 to BES additions and high light levels in our experiments).

338 Alternatively, CH_4 production may be catalyzed by DPOR and COR enzymes.
339 Nitrogenases reduce a range of multi-bond compounds (59, 60, 61, 62, 63), and this quality is
340 shared across different nitrogenases (64). We propose that, similar to the findings of Zheng et al.

341 (62), the nitrogenase-like enzymes DPOR and COR may be able to catalyze the reduction of CO_2
342 into CH_4 when a suitable source of electrons is present. This may explain why BES and high
343 light increased CH_4 production in some experiments, as BES could act as a source of electrons
344 similar to thiosulfate in Zheng et al.'s experiments, while high light levels may disrupt
345 photosynthesis and drive the buildup of electrons and reducing equivalents. Importantly, DPOR
346 and COR are central in photosynthesis, and so are present in Cyanobacteria, as well as within the
347 abundant and ubiquitous freshwater bacterial groups *Limnohabitans* and *Polynucleobacter* (31,
348 33, 52).
349
350 *Multiple co-occurring mechanisms produce methane in aquatic ecosystems*
351 Our combined results indicate that multiple paradoxical CH_4 production mechanisms are active
352 in freshwater ecosystems, and have several implications for our understanding of aquatic CH_4
353 production. First, confirmation of the CH_4 paradox in freshwater is still limited in scope and
354 relatively recent (8, 9, 23), yet freshwater lakes are potentially large sources of CH_4 to the
355 atmosphere (2). We conducted multiple experiments in multiple lakes, and measured significant
356 CH_4 production in controls and/or treatments in 68% of experiments (Fig. 1). In many of the
357 remaining experiments, variations in CH_4 concentrations over time, across experimental
358 treatments, and in *pmoA* gene expression patterns suggest that CH_4 production occurs in parallel
359 with coupled CH_4 oxidation (Fig. 2, SI Text). Because CH_4 oxidation may obscure CH_4
360 production, use of different experimental treatments combined with 'omic data is required to
361 identify paradoxical CH_4 production. Our findings therefore expand on limited data and
362 demonstrate that paradoxical CH_4 production is common, but variable, in freshwater.
363 Given the ubiquity of *phnJ* genes in our data (Fig. 2), their presence on contigs from
364 abundant organisms (Tables S1-S3), and the potential for P limitation, microbial metabolism of
365 MPn may represent an important baseline CH_4 production mechanism in freshwater lakes. This
366 fits with current understanding of marine ecosystems (6, 16). Metatranscriptomic and
367 metagenomic data also indicate that, like the ocean, DMSP transformations may be active in
368 freshwater—with potential implications for both DMS and CH_4 production. Our data further
369 demonstrate that MPn may itself be produced within lakes based on *ppd* and *pepM* expression
370 (Fig. 2). Quantifying the relative contributions of allochthonous vs. autochthonous MPn
371 production—as well as broader P acquisition dynamics—is therefore essential to understanding

372 CH_4 production in freshwater. Phosphonate compounds were once thought to be resistant to
373 breakdown and their formation remains poorly understood (17, 65). Under P limiting conditions,
374 competition for these and other P compounds among multiple groups of organisms will be
375 intense, and potentially variable in space and time. Along with variations in CH_4 oxidation
376 relative to production rates, this can drive variations in CH_4 production such as those evident in
377 our data.

378 As a newly-identified CH_4 source that occurs via an unknown pathway (23), we used a
379 combination of approaches to identify whether photosynthetic CH_4 production occurs in
380 freshwater, and by what means. Although independent data types (CH_4 concentrations, treatment
381 effects, isotopic data, 'omic data) may be interpreted in multiple ways, the combined data are
382 consistent with photosynthetic production in the UC4 experiment (Figs. 3 and 4). For example,
383 the high light and BES treatments boosted CH_4 concentrations (Fig. S2), but this CH_4 is unlikely
384 to have been the result of methanogenesis or MPn breakdown given low and decreasing *mcrA*
385 and *phnJ* expression (Fig. 4). Instead, COR and DPOR transcripts were present and responsive
386 to treatments as shown by metagenomic and metatranscriptomic data. Our data are further
387 indicative of an isotopically light CH_4 source (Fig. 3), which is inconsistent with production from
388 MPn (44, 45) . Extending from the UC4 experiment, photosynthetic CH_4 production may take
389 place in at least five other experiments where BES and high light also significantly increased
390 CH_4 (L2, L3, LG4, UC3, UC4; Fig. S2). Dark treatments further suggest photosynthetic
391 production could occur in several additional experiments alongside increased CH_4 oxidation
392 (Fig. S2). Finally, the ubiquity of COR and DPOR genes and transcripts indicates that the
393 potential for photosynthetic CH_4 production is widespread (Fig. 5), yet the apparent variability
394 across experiments is consistent with known variability in photosynthesis by *Limnohabitans* (51,
395 66).

396 These patterns were most clearly evident in experimental treatments, highlighting the
397 efficacy of including different treatments to examine paradoxical CH_4 production. We leveraged
398 data from these treatments to identify potential CH_4 production mechanisms—providing an
399 experimental approach, isotopic signature data, and two potential gene targets to examine in
400 other aquatic ecosystems. We found that this mechanism is not limited to the Cyanobacteria, as
401 the majority of DPOR and COR transcripts and genes were derived from the betaproteobacteria.
402 This has several important implications. First, *Limnohabitans* and *Polynucleobacter* are among

403 the most abundant and ubiquitous bacteria found in freshwater ecosystems (31). We recovered
404 MAGs from both of these groups, and all contained DPOR and COR genes, as well as genes for
405 phosphonate metabolism. *Limnohabitans* also expressed *phnJ* genes, indicating that they can
406 play a dual role in paradoxical CH_4 production. These findings demonstrate that two
407 mechanisms for paradoxical CH_4 production co-occur in multiple lineages of abundant and
408 widespread bacteria in freshwater. Second, our data are indicative of an additional paradoxical
409 CH_4 production mechanism: CH_4 production by aerobic anoxygenic photosynthetic (AAnP)
410 bacteria. AAnP bacteria are also prevalent in the ocean, where they constitute up to 10% of
411 bacterial communities and play an important role in ocean carbon cycling (66). Given their
412 significance, the potential for CH_4 production by marine AAnP deserves examination. More
413 broadly, COR and DPOR are nitrogenase-like enzymes that have a central role in photosynthesis.
414 Multiple other nitrogenase-like enzymes produce CH_4 (62, 64), and our results implicate COR
415 and DPOR. However, this mechanism is variable across our experiments. This raises the
416 possibility that the potential for photosynthetic CH_4 production is widespread, but not always
417 active. Understanding the factors that regulate photosynthetic CH_4 production (such as light,
418 compounds like BES, and other factors) is therefore important. Our combined dataset
419 consequently demonstrates that paradoxical CH_4 production is complex, with several
420 contributing processes—some present within the same organisms—each affected by a range of
421 environmental variables (e.g., P availability, light), and all producing CH_4 to differing degrees.
422 Understanding this complexity is essential, as multiple paradoxical CH_4 production mechanisms
423 are widely-distributed in aquatic ecosystems, where they may represent important sources of
424 CH_4 to the atmosphere.
425
426 **Materials and Methods**
427
428 *Field site, sample collection, and experimental set up*
429
430 Water samples were collected in 2016-2018 in five high-elevation lakes in Yosemite National
431 Park, and used in incubation experiments. Samples were collected in Lukens (L), Lower
432 Cathedral (LC), Upper Cathedral (UC), Lower Gaylor (LG), and Upper Gaylor (UG) Lakes.
433 Experiments are denoted by lake abbreviation and sequential numbering (Table S5). Water

434 samples were collected in the littoral and limnetic zones of the lakes at 0.1 m depth with acid-
435 washed cubitainers, and then kept on ice or refrigeration to maintain in-lake temperature until
436 laboratory incubations were established within 24 hours of sample collection. Temperature and
437 dissolved oxygen were measured at the time of sample collection using a ProODO YSI probe
438 (YSI Inc., Yellow Springs, OH, USA).

439 Water collected in the lakes was transferred to 170 or 300 ml Wheaton bottles, capped
440 and crimped, and a known volume of air was introduced to generate a headspace for
441 sampling. Initial CH_4 samples were collected, and bottles were incubated in water baths
442 at constant temperature. All incubations were run in triplicate and set to the temperature
443 at which water samples were collected in the field. The different treatments used in the
444 experiments were:

445 - Control: unamended lake water following a natural day-night set up (water bath
446 lid was opened at 7:00 hours and closed at 18:00 hours).
447 - Dark: unamended lake water; bottles were kept in the dark during the whole
448 incubation time.
449 - BES: lake water was amended with 2-bromoethanesulphonate (BES) to a final
450 concentration of $5x10^{-4}$ M. This concentration has been established to inhibit
451 methanogens (25) and has been used in methane paradox experimentation before
452 (8). This treatment followed the same natural daylight set up as the control.
453 - High light: unamended lake water was subjected to 500 mmol/m^2 inside a growth
454 chamber and followed the same natural daylight set up as the control (light would
455 turn on at 7:00 hours and off at 18:00 hours).
456 - Sterile treatments: 0.22 µm-filtered lake water did not show significant CH_4
457 production or oxidation over time, indicating observed CH_4 production and
458 consumption is likely biotic.

459 For all incubation types, gas samples were taken from the headspace every 6-24 hours for up to
460 96 hours with a syringe and immediately transferred to exetainers for later analyses in a gas
461 chromatograph. Not all treatments were tested in each incubation experiment. Temperature and
462 oxygen concentrations were monitored at each sampling point. Optical sensor spots (Fibox,
463 Loligo Systems, Viborg, Denmark) were used to measure oxygen concentrations during
464 incubations (detection limit of 100 nM) and make sure that the water did not go anoxic at any

465 time. Temperature was measured with a Fibox temperature sensor and kept constant during the
466 incubation time. Water samples were filtered at the beginning and end of the incubation for DNA
467 and RNA sampling.
468
469 *Methane measurements*
470 Methane concentrations were measured via headspace equilibration and gas chromatography.
471 Headspace gas samples from incubations were collected with a gas-tight syringe into 12-mL
472 Labco Exetainer vials (Labco Ltd., Lampeter, Ceredigion, UK) after incubations bottles were
473 shaken for 2 minutes to reach equilibration. Samples were subsequently analyzed using a
474 Shimadzu GC-2014 gas chromatograph with flame ionization detection (FID) for CH_4 (67).
475 Headspace CH_4 concentration measurements were then used to calculate CH_4 concentration in
476 lake water based on Henry's law of equilibrium (68).
477
478 *DNA and RNA Extraction*
479 Water samples were filtered through 0.22 µm (Millipore, Darmstadt, Germany) then DNA filter
480 samples were preserved in Sucrose-Tris-EDTA (STE) buffer in pre-prepped Lysis Matrix E
481 tubes and frozen at -80°C until extraction. RNA samples were preserved in RNA*later*®
482 (Ambion™, AM7021) in pre-prepped Lysing Matrix E tubes (MP Bio, Eschwege, Germany),
483 and frozen at -80°C until extraction. DNA was extracted using the Qiagen DNeasy Blood &
484 Tissue Kit with a modified protocol from Beman et al. (69). Briefly, samples were lysed with
485 100µL 10% sodium dodecyl sulfate (SDS), DNA gets separated from proteins and cellular debris
486 using proteinase K (20mg mL^{-1}; Qiagen, Inc., Valencia, CA, USA), precipitated with ethanol and
487 cleaned up. After extraction samples were preserved at -80°C until further analyses. RNA was
488 extracted using a *mir*Vana miRNA Isolation Kit (Ambion™, AM1560) with a modified protocol
489 from Huber and Fortunato (70). Briefly, samples are lysed with the kit's lysing matrix, then
490 subjected to an organic extraction with phenol chloroform followed by a wash to obtain RNA.
491 Immediately after RNA extraction we used the SuperScript III First-Strand Synthesis System for
492 RT-PCR (Life Technologies Corporation, Carlsbad, CA, USA) to synthesize first-strand cDNA
493 and samples were preserved at -80°C until further analyses. DNA, RNA and cDNA purity was
494 measured using a Biospectrometer (Eppendorf AG, Hamburg, Germany) and the concentrations
495 were quantified using PicoGreen Quant-iT dsDNA quantitation assay (ThermoFisher Scientific,

496 USA) for DNA samples and the MaestroNano Pro (Maestrogen Inc., Taiwan) for RNA and
497 cDNA samples.
498
499 *16S sequencing*
500 DNA and RNA extracted from filtered water samples were diluted to a common concentration
501 (1ng/ul) and sent for 16S rRNA amplicon sequencing on an Illumina MiSeq (Illumina, San
502 Diego, CA, USA) according to Earth Microbiome protocols. We used the universal primers
503 515F-Y (5'- GTGYCAGCMGCCGCGGTAA) and 926R (5'-CCGYCAATTYMTTTRAGTTT).
504 DNA samples were sequenced at the Joint Genome Institute (Berkeley, CA, USA) and RNA
505 samples at the Argonne National Laboratory (Lemont, IL, USA).
506 ASVs were generated from 16S rDNA and rRNA sequence data using the Divisive
507 Amplicon Denoising Algorithm (DADA2; 71) as implemented in QIIME 2 (72), and then used
508 for subsequent analyses. After import and demultiplexing, read quality was visualized using the
509 'qiime tools view' command. Reads were then processed using the 'qiime dada2 denoise-paired'
510 command, with 13 bp trimmed from both the forward and reverse reads, truncation of reverse to
511 169 bp (due to the well-known decline in sequence quality observed for MiSeq reverse reads),
512 and training of the denoising algorithm on 1 million reads. Classification of ASVs was
513 conducted in mothur (73) using the SILVA (version 128) database.
514
515 *Metatranscriptomics and metagenomics*
516 Metatranscriptomes and metagenomes were generated from later experiments in order to
517 examine potential production mechanisms and coupled methane oxidation. Following
518 extraction, DNA and RNA samples were sent for metagenome/metatranscriptome sequencing in
519 the Vincent J. Coates Genome Sequencing Laboratory (GSL) at the University of California,
520 Berkeley (https://genomics.qb3.berkeley.edu/), which is supported by NIH S10 OD018174
521 Instrumentation Grant. For each DNA sample, 250 ng of genomic DNA was sheared and
522 libraries were prepared using the KAPA HyperPrep Kit (Kapa Biosystems, Wilmington, MA,
523 USA). For each RNA sample, ~800 ng of total RNA was depleted of rRNA using the Ribo-Zero
524 rRNA Removal Kit (Illumina, Inc., San Diego, CA, USA), sheared, and libraries were prepared
525 using the KAPA RNA HyperPrep Kit (Kapa Biosystems, Wilmington, MA, USA). 12 samples

526 were pooled into a single lane and sequenced via 150-cycle paired-end sequencing on the
527 Illumina HiSeq 4000 platform (Illumina, Inc., San Diego, CA, USA).
528 Data were demultiplexed by the GSL and reads were filtered and trimmed using BBDuk
529 (https://jgi.doe.gov/data-and-tools/bbtools/bb-tools-user-guide/bbduk-guide/) with the following
530 parameters: maq=8, maxns=1, minlen=40,minlenfraction=0.6, k=23, hdist=1, trimq=12,
531 qtrim=rl. Forward and reverse reads were then merged using PANDASeq
532 (https://github.com/neufeld/pandaseq; 74) with default parameters. Merged reads were
533 subsequently annotated in DIAMOND (http://diamondsearch.org/; 75) using the NCBI NR
534 database (accessed February 11th, 2020) with the following search criteria: maximum number of
535 target sequences = 1, bit-score > 40. In order to quantify functional gene abundances, we filtered
536 the DIAMOND annotation data to find the number of functional genes of interest present in each
537 metagenome or metatrascriptome, discarding those with similarity below 60%. We calculated
538 percent abundance based on the total number of reads and the number of targeted genes in each
539 metagenome or metatranscriptome. Metagenomic contigs were assembled via megahit v 1.1.3
540 (76) using an initial k-mer size of 23, and were annotated as described above but with the 'long
541 reads' option in DIAMOND.
542 For additional analyses, UC4 metatranscriptomes were uploaded to the Joint Genome
543 Institute (JGI; https://img.jgi.doe.gov/) Integrated Microbial Genomes & Microbiomes platform
544 for additional analyses. We used the function comparisons tool to identify functions that were
545 significantly different in the treatments vs. the control, and the function category tool identify
546 differences in KEGG pathway categories among the treatments. Moreover, we used the
547 phylogenetic distribution tool to quantify the abundance of different phylogenetic groups of
548 potential importance in the methane paradox. Metatranscriptome reads were also mapped to
549 MAGs using bowtie2 v 2.3.4.3 (77) and visualized using Anvi'o (78). Coverage files were
550 generated in samtools v 1.11 (http://www.htslib.org/) for statistical comparisons. MAGs were
551 assembled as described by Nayfach et al. (53).
552
553 *Stable isotopic measurements*
554 Headspace of incubation bottles was transferred to evacuated exetainers and sent to the UC
555 Davis Stable Isotope Facility (Davis, CA) for analysis. Measurements of stable isotope ratios of
556 carbon ($\delta^{13}C$) in CH_4 were conducted using a ThermoScientific Precon concentration unit

557 interfaced to a ThermoScientific Delta V Plus isotope ratio mass spectrometer
558 (ThermoScientific, Bremen, Germany). In brief, gas samples are passed through a H_2O/CO_2
559 scrubber and a cold trap, and CH_4 is then separated from other gases and oxidized to CO_2. Pure
560 CO_2 reference gas is used to calculate provisional δ values, and final δ values are calculated after
561 correcting for changes in linearity and instrumental drift, and expressed relative to the Vienna
562 PeeDee Belemnite (V-PDB) standard.
563
564 *Statistical analyses*
565 Spearman's correlation test was used to assess the relationship between time (h) and CH_4
566 concentration in all incubations and across all treatments. A priori significance level was defined
567 as $\alpha<0.05$. A significantly positive relationship between time and CH_4 was considered as net CH_4
568 production in the incubation, whereas a significantly negative relationship was considered as net
569 CH_4 consumption; otherwise we defined the incubation as not having significant net production
570 or consumption over time. We subsequently used ANOVA and Tukey honestly significant
571 difference (HSD) post-hoc tests to test for cases where CH_4 production or oxidation varied
572 significantly between sampling time points, resulting in nonlinear patterns in CH_4 concentrations
573 over the course of the experiment. For example, initial CH_4 production could be followed by
574 subsequent oxidation, resulting in significant CH_4 increases followed by significant decreases.
575 To express the different responses in terms of CH_4 concentration over time among the
576 different experiments treatments we first calculated the response ratios (lnRR) by the
577 following equation:
578
579 $$lnRR = ln\ \frac{mean\ CH_4\ in\ treatment}{mean\ CH_4\ in\ control}$$
580
581 Additionally, we calculated which treatments were significantly different from each other
582 and the control using ANOVA and Tukey honestly significant difference (HSD) post-hoc
583 tests. All statistical analyses and figures were done in the R statistical environment
584 (RStudioVersion 1.2.5001).
585
586

References

1. IPCC, Climate change 2014: Synthesis report. Contribution of working groups I, II, and III to the fifth assessment report of the intergovernmental panel on climate change" (IPCC, Geneva 2014)

2. D. Bastviken, J. Cole, M. Pace, L. Tranvik, Methane emissions from lakes: Dependence of lake characteristics, two regional assessments, and a global estimate. *Global Biogeochemical Cycles* **18** (2004).

3. D. Bastviken, "Methane" in *Encyclopedia of Inland Waters*, G. E. Likens, Ed. (Academic Press, 2009), pp. 783–805.

4. K. W. Tang, D. F. McGinnis, D. Ionescu, H.-P. Grossart, Methane Production in Oxic Lake Waters Potentially Increases Aquatic Methane Flux to Air. *Environ. Sci. Technol. Lett.* **3**, 227–233 (2016).

5. T. Hoehler, N. A. Losey, R. P. Gunsalus, M. J. McInerney, "Environmental Constraints that Limit Methanogenesis [Reference work chapter]" (Springer, 2018).

6. D. M. Karl, *et al.*, Aerobic production of methane in the sea. *Nature Geoscience* **1**, 473–478 (2008).

7. E. Damm, *et al.*, Methane production in aerobic oligotrophic surface water in the central Arctic Ocean. *Biogeosciences* **7**, 1099–1108 (2010).

8. H.-P. Grossart, K. Frindte, C. Dziallas, W. Eckert, K. W. Tang, Microbial methane production in oxygenated water column of an oligotrophic lake. *PNAS* **108**, 19657–19661 (2011).

9. M. J. Bogard, *et al.*, Oxic water column methanogenesis as a major component of aquatic CH_4 fluxes. *Nature Communications* **5**, 5350 (2014).

10. K. W. Tang, D. F. McGinnis, K. Frindte, V. Brüchert, H.-P. Grossart, Paradox reconsidered: Methane oversaturation in well-oxygenated lake waters. *Limnology and Oceanography* **59**, 275–284 (2014).

11. J. C. Angle, *et al.*, Methanogenesis in oxygenated soils is a substantial fraction of wetland methane emissions. *Nature Communications* **8**, 1567 (2017).

12. R. S. Oremland, Methanogenic activity in plankton samples and fish intestines A mechanism for in situ methanogenesis in oceanic surface waters. *Limnology and Oceanography* **24**, 1136–1141 (1979).

13. M. A. de Angelis, C. Lee, Methane production during zooplankton grazing on marine phytoplankton. *Limnology and Oceanography* **39**, 1298–1308 (1994).

14. D. M. Karl, B. D. Tilbrook, Production and transport of methane in oceanic particulate organic matter. *Nature* **368**, 732–734 (1994).

15. D. Donis, *et al.*, Full-scale evaluation of methane production under oxic conditions in a mesotrophic lake. *Nature Communications* **8**, 1–12 (2017).

16. D. J. Repeta, *et al.*, Marine methane paradox explained by bacterial degradation of dissolved organic matter. *Nature Geoscience* **9**, 884–887 (2016).

17. S. V. Kononova, M. A. Nesmeyanova, Phosphonates and Their Degradation by Microorganisms. *Biochemistry (Moscow)* **67**, 184–195 (2002).

18. J. Huang, Z. Su, Y. Xu, The Evolution of Microbial Phosphonate Degradative Pathways. *J Mol Evol* **61**, 682–690 (2005).

19. O. A. Sosa, D. J. Repeta, E. F. DeLong, M. D. Ashkezari, D. M. Karl, Phosphate-limited ocean regions select for bacterial populations enriched in the carbon–phosphorus lyase pathway for phosphonate degradation. *Environmental Microbiology* **21**, 2402–2414 (2019).

20. M. Yao, C. Henny, J. A. Maresca, Freshwater Bacteria Release Methane as a By-Product of Phosphorus Acquisition. *Appl. Environ. Microbiol.* **82**, 6994–7003 (2016).

21. Q. Wang, J. E. Dore, T. R. McDermott, Methylphosphonate metabolism by Pseudomonas sp. populations contributes to the methane oversaturation paradox in an oxic freshwater lake. *Environmental Microbiology* **19**, 2366–2378 (2017).

22. W. Li, *et al.*, Methane production in the oxygenated water column of a perennially ice-covered Antarctic lake. *Limnology and Oceanography* **65**, 143–156 (2020).

23. M. Bižić, *et al.*, Aquatic and terrestrial cyanobacteria produce methane. *Science Advances* **6**, eaax5343 (2020).

24. M. Günthel, *et al.*, Photosynthesis-driven methane production in oxic lake water as an important contributor to methane emission. *Limnology and Oceanography* **n/a**.

25. R. S. Oremland, D. G. Capone, "Use of 'Specific' Inhibitors in Biogeochemistry and Microbial Ecology" in *Advances in Microbial Ecology*, Advances in Microbial Ecology., K. C. Marshall, Ed. (Springer US, 1988), pp. 285–383.

26. S. S. Rizk, M. J. Cuneo, H. W. Hellinga, Identification of cognate ligands for the Escherichia coli phnD protein product and engineering of a reagentless fluorescent biosensor for phosphonates. *Protein Science* **15**, 1745–1751 (2006).

27. X. Yu, *et al.*, Diversity and abundance of phosphonate biosynthetic genes in nature. *Proc. Natl. Acad. Sci. U.S.A.* **110**, 20759–20764 (2013).

28. R. P. Kiene, L. J. Linn, J. A. Bruton, New and important roles for DMSP in marine microbial communities. *Journal of Sea Research* **43**, 209–224 (2000).

29. M. A. Moran, C. R. Reisch, R. P. Kiene, W. B. Whitman, Genomic Insights into Bacterial DMSP Transformations. *Annual Review of Marine Science* **4**, 523–542 (2012).

30. M. Sela-Adler, *et al.*, Isotopic evidence for the origin of dimethylsulfide and dimethylsulfoniopropionate-like compounds in a warm, monomictic freshwater lake. *Environ. Chem.* **13**, 340–351 (2015).

31. R. J. Newton, S. E. Jones, A. Eiler, K. D. McMahon, S. Bertilsson, A Guide to the Natural History of Freshwater Lake Bacteria. *Microbiol. Mol. Biol. Rev.* **75**, 14–49 (2011).

32. V. Kasalický, J. Jezbera, M. W. Hahn, K. Šimek, The Diversity of the Limnohabitans Genus, an Important Group of Freshwater Bacterioplankton, by Characterization of 35 Isolated Strains. *PLoS One* **8** (2013).

33. J. F. Imhoff, T. Rahn, S. Künzel, S. C. Neulinger, Phylogeny of Anoxygenic Photosynthesis Based on Sequences of Photosynthetic Reaction Center Proteins and a Key Enzyme in Bacteriochlorophyll Biosynthesis, the Chlorophyllide Reductase. *Microorganisms* **7**, 576 (2019).

34. K. M. Björkman, D. M. Karl, Bioavailability of dissolved organic phosphorus in the euphotic zone at Station ALOHA, North Pacific Subtropical Gyre. *Limnology and Oceanography* **48**, 1049–1057 (2003).

35. J. O. Sickman, J. M. Melack, D. W. Clow, Evidence for nutrient enrichment of high-elevation lakes in the Sierra Nevada, California. *Limnology and Oceanography* **48**, 1885–1892 (2003).

36. J. J. Elser, *et al.*, Shifts in Lake N:P Stoichiometry and Nutrient Limitation Driven by Atmospheric Nitrogen Deposition. *Science* **326**, 835–837 (2009).

37. K. A. Moser, *et al.*, Mountain lakes: Eyes on global environmental change. *Global and Planetary Change* (2019) https:/doi.org/10.1016/j.gloplacha.2019.04.001 (April 19, 2019).

38. C. J. Hayden, J. M. Beman, Microbial diversity and community structure along a lake elevation gradient in Yosemite National Park, California, USA. *Environmental Microbiology* **18**, 1782–1791 (2016).

39. E. Perez-Coronel, S. C. Hart, J. M. Beman, Seasonal methane dynamics in high-elevation lakes in the Sierra Nevada California: the role of elevation, temperature, organic matter, and inorganic nutrients. EarthArXiv: https:/doi.org/10.31223/osf.io/yvgq4 (06 July 2020).

40. J. F. Dumestre, *et al.*, Influence of Light Intensity on Methanotrophic Bacterial Activity in Petit Saut Reservoir, French Guiana. *Appl. Environ. Microbiol.* **65**, 534–539 (1999).

41. J. Murase, A. Sugimoto, Inhibitory effect of light on methane oxidation in the pelagic water column of a mesotrophic lake (Lake Biwa, Japan). *Limnology and Oceanography* **50**, 1339–1343 (2005).

42. S. D. Thottathil, P. C. J. Reis, P. A. del Giorgio, Y. T. Prairie, The Extent and Regulation of Summer Methane Oxidation in Northern Lakes. *Journal of Geophysical Research: Biogeosciences* **123**, 3216–3230 (2018).

43. J. Grey, The Incredible Lightness of Being Methane-Fuelled: Stable Isotopes Reveal Alternative Energy Pathways in Aquatic Ecosystems and Beyond. *Front. Ecol. Evol.* **4** (2016).

44. L. Taenzer, *et al.*, Microbial Methane From Methylphosphonate Isotopically Records Source. *Geophysical Research Letters* **47**, e2019GL085872 (2020).

45. J. H. Street, R. S. Anderson, A. Paytan, An organic geochemical record of Sierra Nevada climate since the LGM from Swamp Lake, Yosemite. *Quaternary Science Reviews*. **40**, 89–106 (2012).

46. J. F. Hartmann, *et al.*, High Spatiotemporal Dynamics of Methane Production and Emission in Oxic Surface Water. *Environ. Sci. Technol.* **54**, 1451–1463 (2020).

47. Y. Fujita, H. Matsumoto, Y. Takahashi, H. Matsubara, Identification of a nifDK-Like Gene (ORF467) Involved in the Biosynthesis of Chlorophyll in the Cyanobacterium Plectonema boryanum. *Plant Cell Physiol* **34**, 305–314 (1993).

48. J. Nomata, T. Ogawa, M. Kitashima, K. Inoue, Y. Fujita, NB-protein (BchN-BchB) of dark-operative protochlorophyllide reductase is the catalytic component containing oxygen-tolerant Fe-S clusters. *FEBS Letters* **582**, 1346–1350 (2008).

49. J. Nomata, T. Mizoguchi, H. Tamiaki, Y. Fujita, A Second Nitrogenase-like Enzyme for Bacteriochlorophyll Biosynthesis Reconstitution of Chlorophyllide a Reductase with Purified X-protein (BchX) and YZ-protein (BchY-BchZ) from Rhodobacter Capsulatus. *J. Biol. Chem.* **281**, 15021–15028 (2006).

50. A. G. M. Chew, D. A. Bryant, Chlorophyll Biosynthesis in Bacteria: The Origins of Structural and Functional Diversity. *Annual Review of Microbiology* **61**, 113–129 (2007).

51. Y. Tsukatani, *et al.*, An unexpectedly branched biosynthetic pathway for bacteriochlorophyll b capable of absorbing near-infrared light. *Sci Rep* **3** (2013).

52. V. Kasalický, *et al.*, Aerobic Anoxygenic Photosynthesis Is Commonly Present within the Genus Limnohabitans. *Appl. Environ. Microbiol.* **84** (2018).

53. S. Nayfach, S. Roux, R. Seshadri, D. Udwary, N. Varghese, F. Schulz, D. Wu, D. Paez-Espino, I.-M. Chen, M. Huntemann, K. Palaniappan, J. Ladau, S. Mukherjee, T. B. K. Reddy, T. Nielsen, E. Kirton, J. P. Faria, J. N. Edirisinghe, C. S. Henry, S. P. Jungbluth, D. Chivian, P. Dehal, E. M. Wood-Charlson, A. P. Arkin, S. G. Tringe, A. Visel, T. Woyke, N. J. Mouncey, N. N. Ivanova, N. C. Kyrpides, E. A. Eloe-Fadrosh, A genomic catalog of Earth's microbiomes. *Nature Biotechnology*, 1–11 (2020).

54. F. Keppler, J. T. G. Hamilton, M. Braß, T. Röckmann, Methane emissions from terrestrial plants under aerobic conditions. *Nature* **439**, 187–191 (2006).

55. D. J. Messenger, A. R. Mcleod, S. C. Fry, The role of ultraviolet radiation, photosensitizers, reactive oxygen species and ester groups in mechanisms of methane formation from pectin. *Plant, Cell & Environment* **32**, 1–9 (2009).

56. I. Vigano, *et al.*, Effect of UV radiation and temperature on the emission of methane from plant biomass and structural components. *Biogeosciences* **5**, 937–947 (2008).

57. D. Bruhn, I. M. Møller, T. N. Mikkelsen, P. Ambus, Terrestrial plant methane production and emission. *Physiologia Plantarum* **144**, 201–209 (2012).

58. F. Keppler, *et al.*, Methoxyl groups of plant pectin as a precursor of atmospheric methane: evidence from deuterium labelling studies. *New Phytologist* **178**, 808–814 (2008).

59. Y. Hu, C. C. Lee, M. W. Ribbe, Extending the Carbon Chain: Hydrocarbon Formation Catalyzed by Vanadium/Molybdenum Nitrogenases. *Science* **333**, 753–755 (2011).

60. Z.-Y. Yang, D. R. Dean, L. C. Seefeldt, Molybdenum Nitrogenase Catalyzes the Reduction and Coupling of CO to Form Hydrocarbons. *J. Biol. Chem.* **286**, 19417–19421 (2011).

61. C. C. Lee, Y. Hu, M. W. Ribbe, Vanadium Nitrogenase Reduces CO. *Science* **329**, 642–642 (2010).

62. Y. Zheng, *et al.*, A pathway for biological methane production using bacterial iron-only nitrogenase. *Nature Microbiology* **3**, 281–286 (2018).

63. J. A. North, A. B. Narrowe, W. Xiong, K. M. Byerly, G. Zhao, S. J. Young, S. Murali, J. A. Wildenthal, W. R. Cannon, K. C. Wrighton, R. L. Hettich, F. R. Tabita, A nitrogenase-like enzyme system catalyzes methionine, ethylene, and methane biogenesis. *Science*. **369**, 1094–1098 (2020).

64. L. C. Seefeldt, *et al.*, Reduction of Substrates by Nitrogenases. *Chem. Rev.* **120**, 5082–5106 (2020).

65. P. Kafarski, Phosphonates: Their Natural Occurrence and Physiological Role. *Contemporary Topics about Phosphorus in Biology and Materials* (2019).

66. M. Koblížek, Ecology of aerobic anoxygenic phototrophs in aquatic environments. *FEMS Microbiology Reviews*. **39**, 854–870 (2015).

67. R. F. Weiss, Determinations of Carbon Dioxide and Methane by Dual Catalyst Flame Ionization Chromatography and Nitrous Oxide by Electron Capture Chromatography. *J Chromatogr Sci* **19**, 611–616 (1981).

68. S. Yamamoto, J. B. Alcauskas, T. E. Crozier, Solubility of methane in distilled water and seawater. *J. Chem. Eng. Data* **21**, 78–80 (1976).

763 69. J. M. Beman, B. N. Popp, S. E. Alford, Quantification of ammonia oxidation rates and
764 ammonia-oxidizing archaea and bacteria at high resolution in the Gulf of California and
765 eastern tropical North Pacific Ocean. *Limnology and Oceanography* **57**, 711–726 (2012).

766 70. J. Huber, RNA Extraction Protocol from RNA-SIP Experiments (2017)
767 https:/doi.org/10.17504/protocols.io.iuycexw (May 6, 2020).

768 71. B. J. Callahan, *et al.*, DADA2: High-resolution sample inference from Illumina amplicon
769 data. *Nature Methods* **13**, 581–583 (2016).

770 72. E. Bolyen, *et al.*, Reproducible, interactive, scalable and extensible microbiome data
771 science using QIIME 2. *Nature Biotechnology* **37**, 852–857 (2019).

772 73. P. D. Schloss, *et al.*, Introducing mothur: Open-Source, Platform-Independent, Community-
773 Supported Software for Describing and Comparing Microbial Communities. *Appl. Environ.*
774 *Microbiol.* **75**, 7537–7541 (2009).

775 74. A. P. Masella, A. K. Bartram, J. M. Truszkowski, D. G. Brown, J. D. Neufeld, PANDAseq:
776 paired-end assembler for illumina sequences. *BMC Bioinformatics* **13**, 31 (2012).

777 75. B. Buchfink, C. Xie, D. H. Huson, Fast and sensitive protein alignment using DIAMOND.
778 *Nature Methods* **12**, 59–60 (2015).

779 76. D. Li, R. Luo, C.-M. Liu, C.-M. Leung, H.-F. Ting, K. Sadakane, H. Yamashita, T.-W.
780 Lam, MEGAHIT v1.0: A fast and scalable metagenome assembler driven by advanced
781 methodologies and community practices. *Methods*. **102**, 3–11 (2016).
782
783 77. B. Langmead, S. L. Salzberg, Fast gapped-read alignment with Bowtie 2. *Nature Methods*.
784 **9**, 357–359 (2012).
785
786 78. A. M. Eren, Ö. C. Esen, C. Quince, J. H. Vineis, H. G. Morrison, M. L. Sogin, T. O.
787 Delmont, Anvi'o: an advanced analysis and visualization platform for 'omics data. *PeerJ*.
788 **3**, e1319 (2015).
789

Acknowledgments and funding sources

This work was supported by the University of California through the Valentine Eastern Sierra Reserve graduate student research grant, the Institute for the Study of Ecological and Evolutionary Climate Impacts fellowship, the University of California Merced Environmental Systems summer grants, and the UC MEXUS-CONACYT doctoral fellowship. We thank the United States National Park Service for facilitating sample collection in Yosemite National Park under permits YOSE-2016-SCI-0118, YOSE-2017-SCI-0104 and YOSE-2018-SCI-0091. We thank Steve Hart for his help processing methane samples, Jay Sexton for his help with incubation chambers, and Angela Yu, Joaquin Fraga, Sonia Vargas, Ariadna Cairo, Samantha Vazquez, Jorge Montiel and Daniela Alonso for their help with field and laboratory work.

Figures and Tables

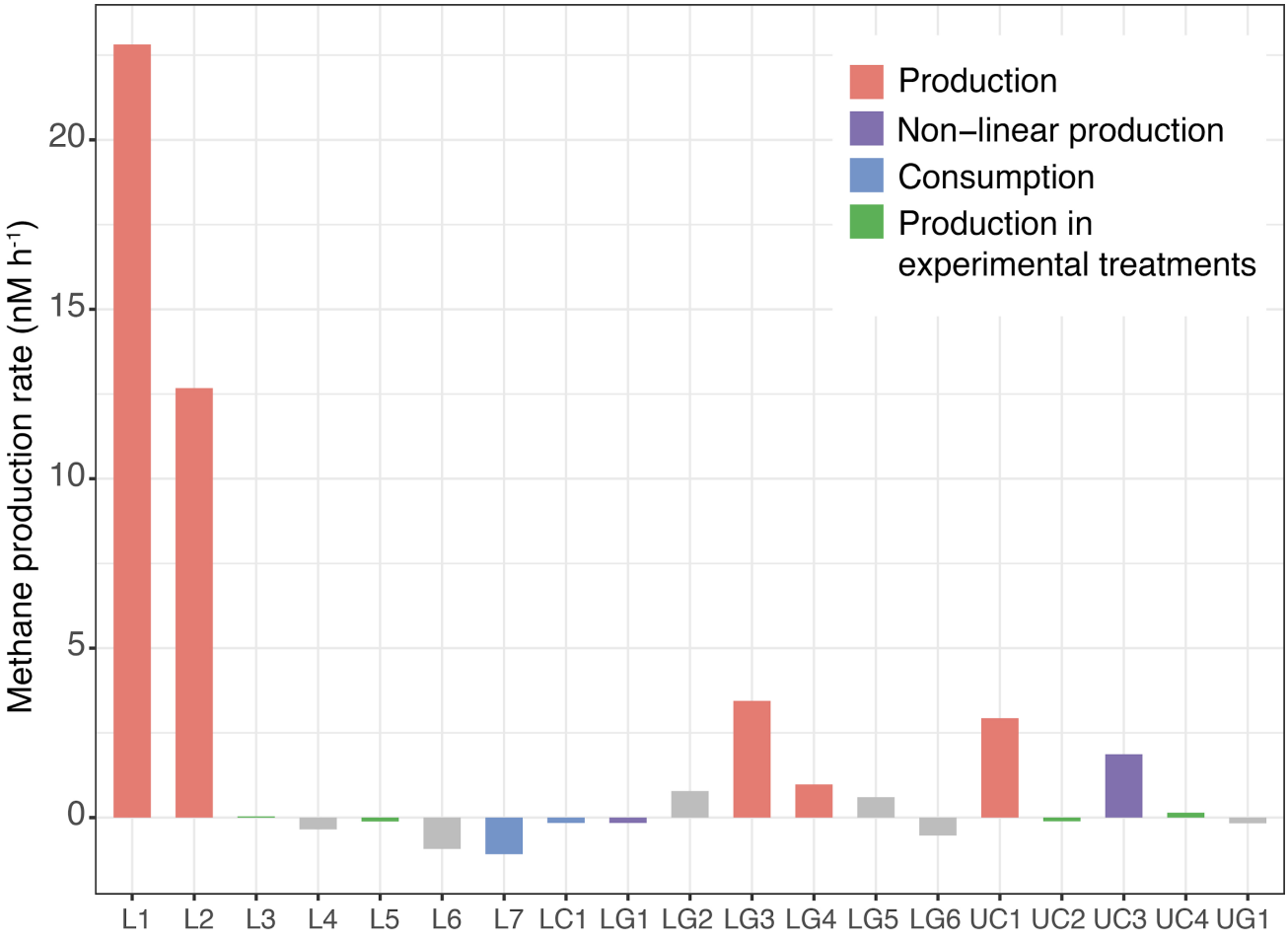

Fig. 1. Net methane (CH_4) production or consumption rates over 24 hours in unamended controls from each experiment. Different colors represent significant linear increases (production; red), linear decreases (consumption; blue), significant nonlinear patterns (purple), production in at least one treatment (green), or no significant change in CH_4 concentrations (grey). Abbreviations denote lake and experiment number (e.g., UC4 is the fourth experiment in Upper Cathedral lake).

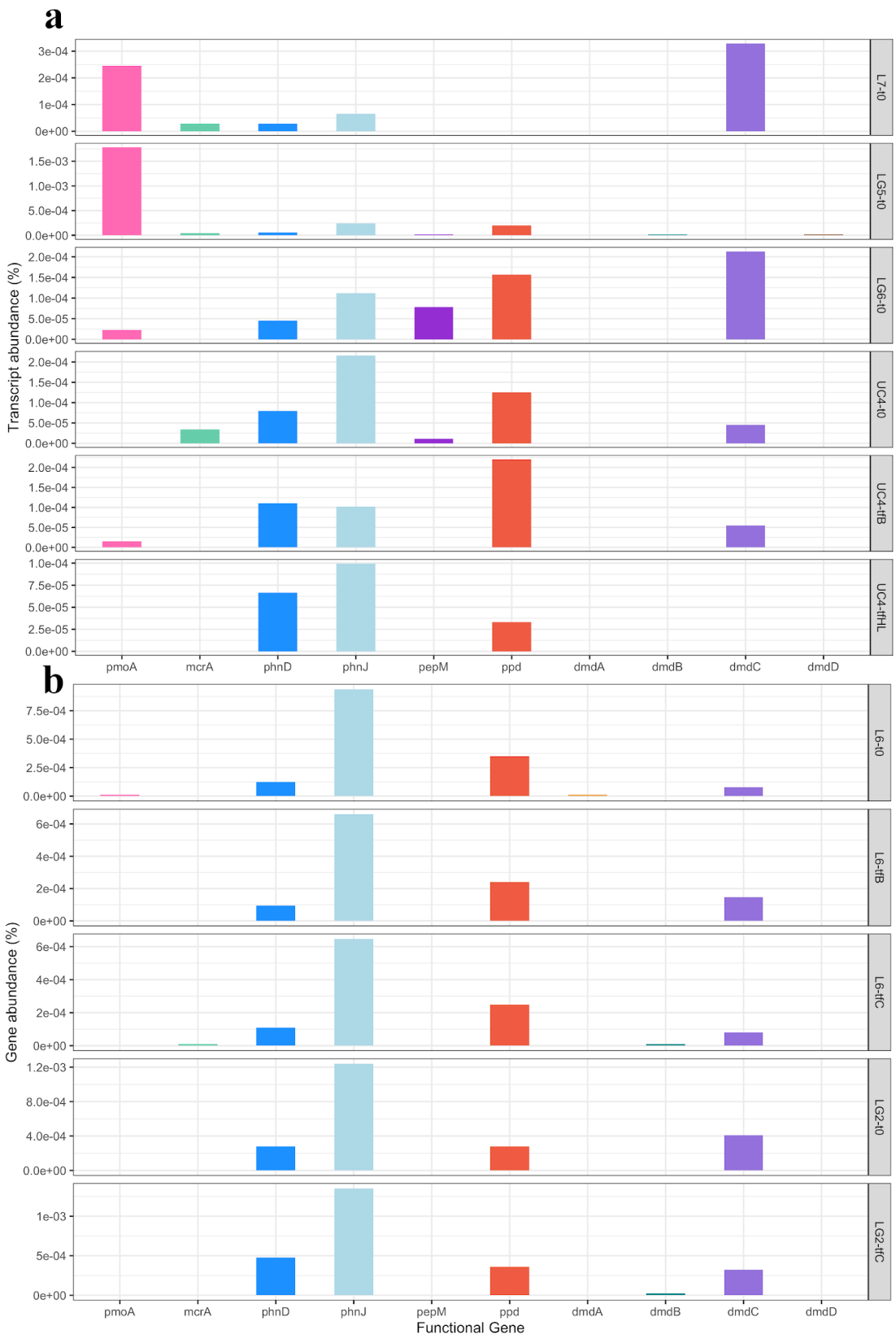
a
Transcript abundance (%)
L7-t0
LG5-t0
LG6-t0
UC4-t0
UC4-tfB
UC4-tfHL
pmoA
mcrA
phnD
phnJ
pepM
ppd
dmdA
dmdB
dmdC
dmdD
b
Gene abundance (%)
L6-t0
L6-tfB
L6-tfC
LG2-t0
LG2-tfC
Functional Gene

813

814 **Fig. 2.** Variations across experiments and treatments in (a) transcript abundance (% of total reads
815 of metatranscriptomes) and (b) gene abundance (% of total reads of metagenomes) of key
816 functional genes. Functional genes quantified included those involved in: methane oxidation
817 (*pmoA*), methanogenesis (*mcrA*), phosphonate assimilation (*phnD*, *phnJ*) and production (*ppd*,
818 *pepM*), and DMSP metabolism (*dmdA*, *dmdB*, *dmdC*, *dmdD*).
819

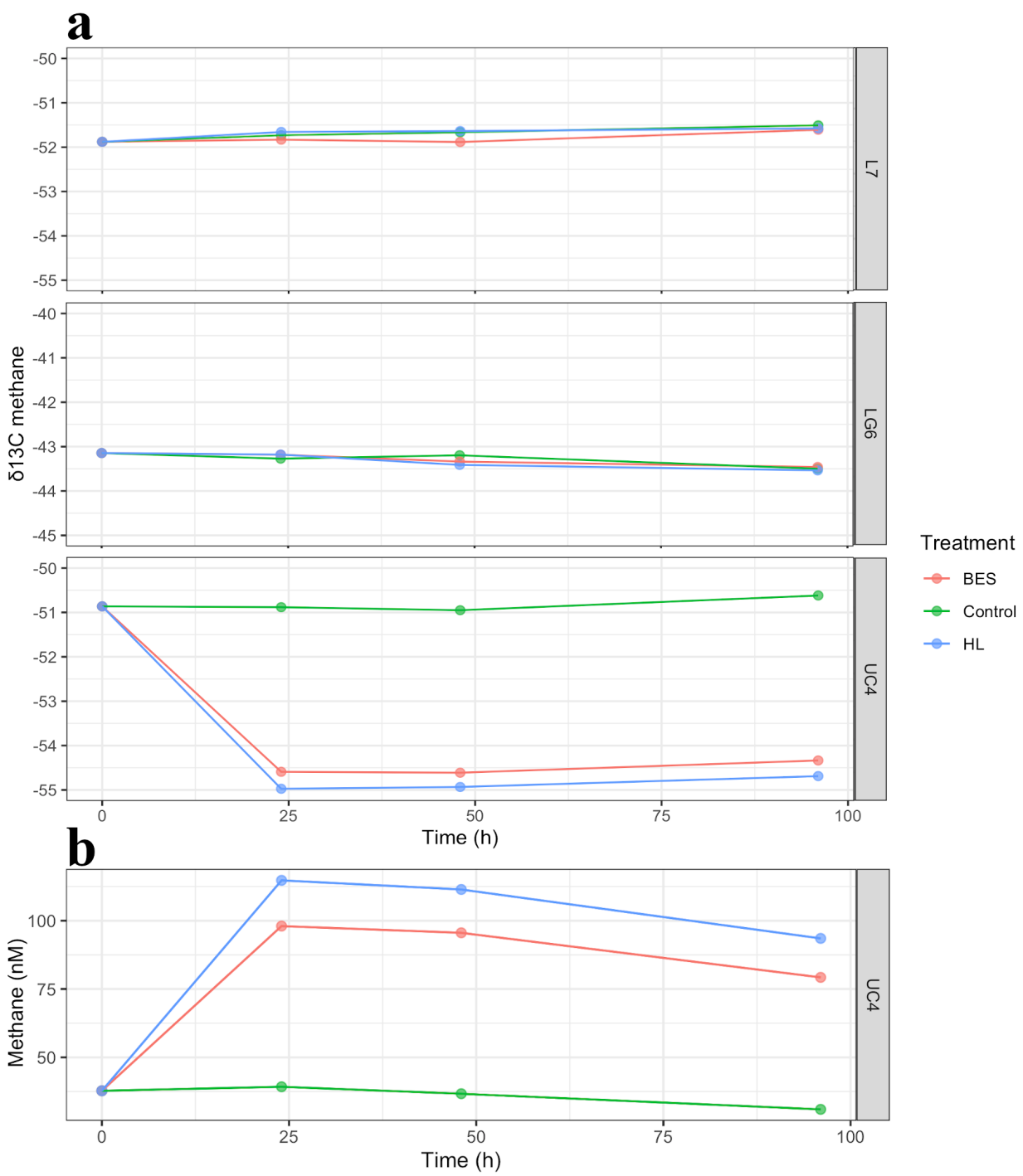

Fig. 3. CH_4 (a) $\delta^{13}C$ values over time in the L7, LG6, and UC4 experiments and (b) concentrations over time in UC4 experiment. Different colors denote different experimental treatments. Scales of the vertical axes differ between experiments in panel a.

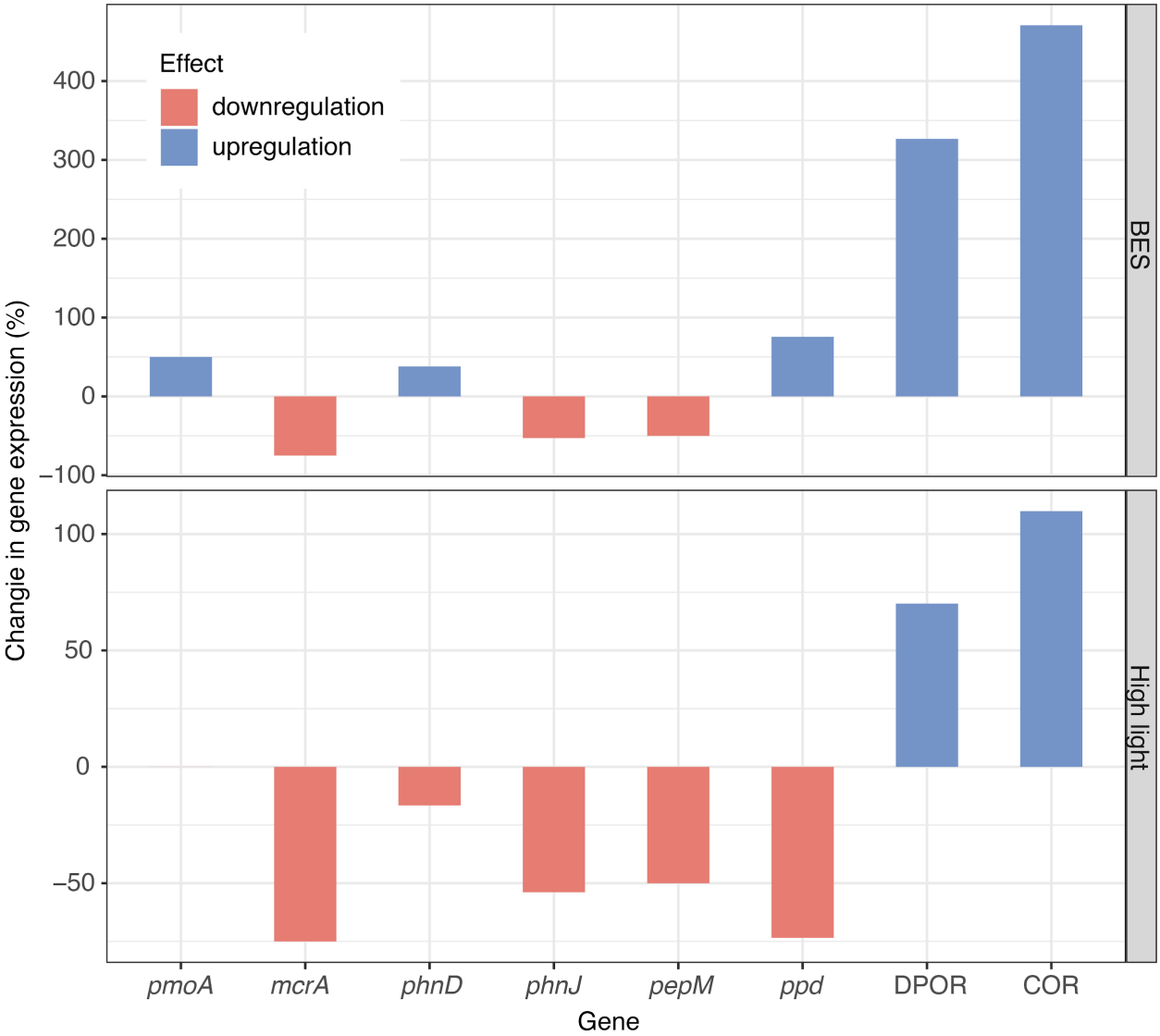

Fig. 4. Upregulation and downregulation of genes involved in methane oxidation (*pmoA*), methanogenesis *(mcrA*), phosphonate assimilation (*phnD*, *phnJ*) and synthesis (*pepM*, *ppd*), and porphyrin and chlorophyll metabolism (DPOR and COR) in the UC4 experiment. BES treatment is shown in the top panel and the high-light treatment in the bottom panel. Colors denote the net effect of the treatment on the different genes in metatranscriptomes.

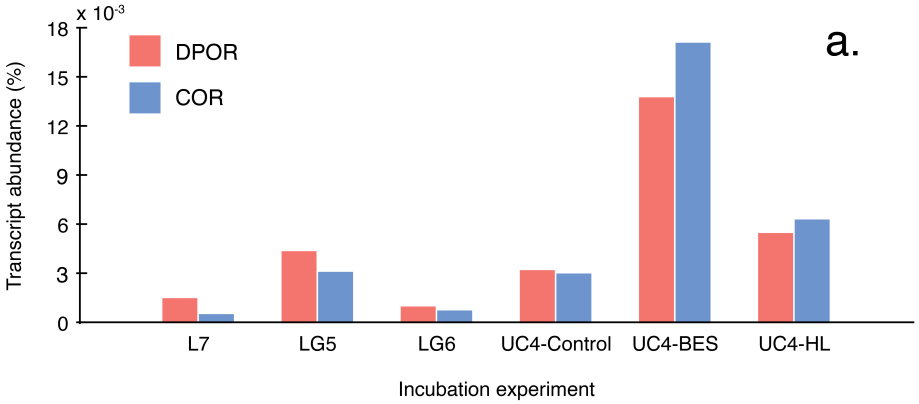
a.
x 10-3
18
15
12
9
6
3
0
Transcript abundance (%)
DPOR
COR
L7
LG5
LG6
UC4-Control
UC4-BES
UC4-HL
Incubation experiment

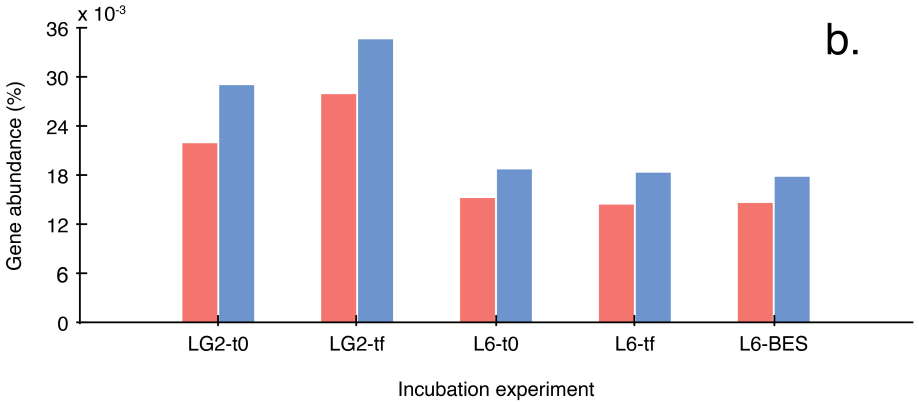
b.
x 10-3
36
30
24
18
12
6
0
Gene abundance (%)
LG2-t0
LG2-tf
L6-t0
L6-tf
L6-BES
Incubation experiment

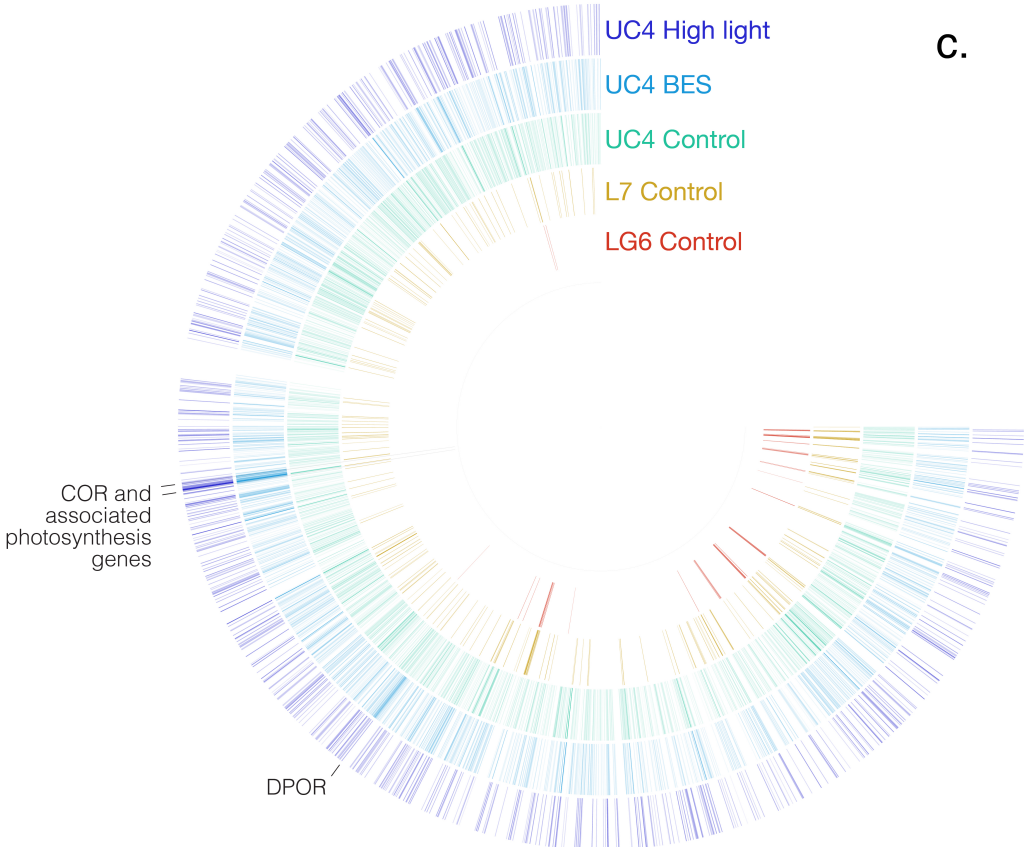
c.
UC4 High light
UC4 BES
UC4 Control
L7 Control
LG6 Control
COR and associated photosynthesis genes
DPOR

833

834 **Fig. 5.** DPOR and COR reads in (a) metatranscriptomes, (b) metagenomes, and (c) mapped to
835 the *Limnohabitans* metagenome-assembled genome (MAG) 5. In panels a and b, DPOR (red)
836 and COR (blue) transcripts (a) and genes (b) are shown within different experiments and
837 experimental treatments. In panel c, the *Limnohabitans* MAG 5 is shown in circular form, and
838 the number of reads mapping to genes within the MAG are indicated by color intensity. The
839 LG6 experiment is shown in red, L7 in orange, UC4 control in aqua, UC4 BES in light blue, and
840 UC4 high-light in dark blue. Locations of DPOR and COR (and associated photosynthesis
841 genes) within the MAG are indicated.
842

843 **Table 1**. Relative abundance of methanogens, Cyanobacteria, and *Comamonadaceae* as a % of
844 16S rRNA genes and transcripts sequenced in different experiments and treatments
845

Exp.	Treatment	Time (h)	Methanogens	Cyanobacteria	*Comamonadaceae*
			% of 16S rRNA genes		
L1	Control	0	0	0.902	9.17
L2	Control	0	0	1.10	6.03
	Control	24	0	1.65	5.20
L3	Control	0	0	0.061	4.56
L4	Control	0	0	2.38	7.97
L6	Control	0	0	5.55	2.03
	BES	45	0	12.6	0.338
LG1	Control	0	0	0.646	5.32
	Control	24	0	0.377	2.04
LG2	Control	0	0	0.795	11.1
LG3	Control	24	0	0.246	0.881
LG4	Control	0	0	5.79	4.35
UC1	Control	0	0	0.880	11.6
			% of 16S rRNA transcripts		
L5	Control	0	0	46.0	6.43
	Control	74	0	28.8	6.66
	Dark	74	0.014	58.5	4.70
	BES	74	0	24.9	8.65
L6	Control	0	0	8.34	6.27
	Control	55	0	0.800	5.42
	BES	55	0	0	5.20
L7	Dark	96	0	65.5	0.841
	BES	96	0	46.4	1.95
	High light	96	0	45.0	1.06
LG5	Control	0	0	17.3	12.8
	Control	86	0	2.00	12.0
	Dark	86	0.008	19.2	10.2
	BES	86	0	1.04	25.6
LG6	Control	0	0	3.05	6.14
	Control	96	0	2.45	8.69
	Dark	96	0	2.65	2.53
	BES	96	0	2.28	5.02
	High light	96	0	7.18	2.64
UC3	Control	0	0	0.227	7.98
	Control	24	0	0.275	8.72
	Control	48	0	0.221	15.2
	Control	57	0	0	12.3
	Dark	57	0	0	8.66
	BES	57	0	0	10.9
UC4	Control	96	0	3.148	14.0
	High light	96	0	0.474	7.25

846

Supplementary Materials for

Biogeochemical and omic evidence for paradoxical methane production via multiple co-occurring mechanisms in aquatic ecosystems

Elisabet Perez-Coronel*, J. Michael Beman

*Corresponding author. Email: elisabetperezcoronel@gmail.com

This PDF file includes:

Supplementary text
Figures S1 and S2
Tables S1 to S5
SI References

Supplementary Information Text

Methane production and consumption over time

All experiments were conducted for at least 24 hours to permit direct comparisons across experiments. However, we included multiple sampling time points before 24 hours in some experiments, while others were conducted for up to 96 hours (Fig. S1). Although longer incubations may introduce bottle effects, this has been used in earlier work (1, 2), and provides multiple comparisons through time, between treatments, and across experiments.

In experiments with multiple sampling time points before 24 hours, we occasionally observed initial decreases that were followed by increases by 24 hours (Fig. S1). This could be explained by the development of P limitation that triggers methane (CH_4) production; for example, Karl et al. (3) observed CH_4 production by MPn breakdown only under P-stressed conditions. Other incubations showed the opposite pattern: an initial increase followed by a decrease in concentration (L2, UC2, LG1). Longer experiments likewise showed eventual decreases in CH_4 concentrations after 24 hours (e.g., L4, L7, LC1, UC4). This behavior has been observed in earlier studies (4) and was the intention of these experiments; specifically, longer incubations may capture the time lag between initial production followed by eventual consumption once CH_4 concentrations exceed a required threshold for methanotrophy. Put another way, both CH_4 production and consumption are taking place, but production rates exceed oxidation rates until oxidation 'catches up' and eventually exceeds production. In general, *pmoA* transcripts were more abundant when CH_4 concentrations in the incubations were higher (L7, LG5 and LG6; CH_4 >100 nM)—consistent with threshold-dependent CH_4 oxidation (4). A similar pattern was evident in metagenomes, as *pmoA* genes were absent in the LG2 incubations where the CH_4 concentrations were <50 nM, and in low abundance in the L6 incubations (CH_4 = ~100 nM).

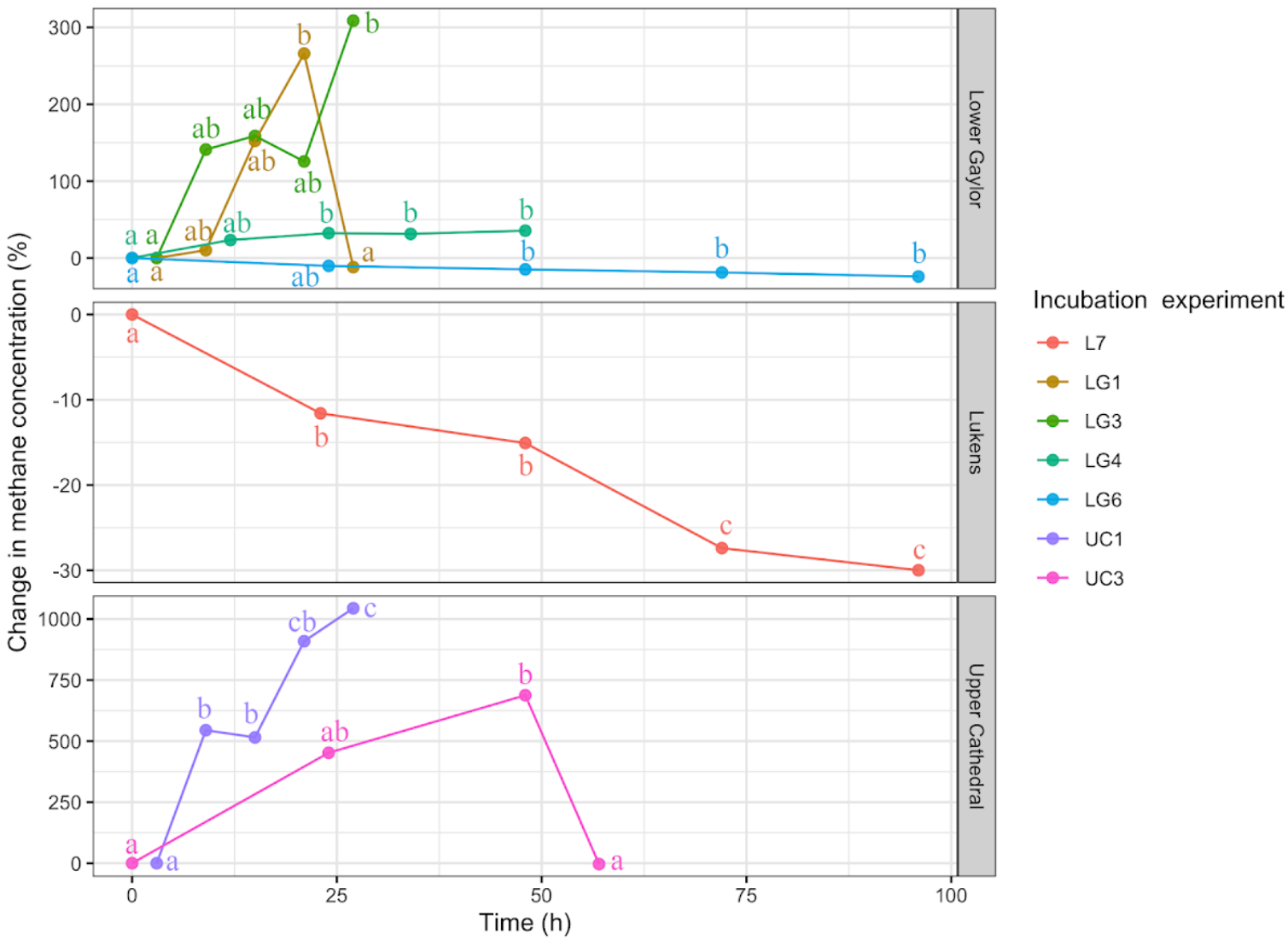

Fig. S1. Percent change in methane (CH_4) concentrations over time. Different colors represent each incubation experiment with statistically significant differences in CH_4 concentrations among different time points. Letters represent similarities or differences between time points according to Tukey HSD test.

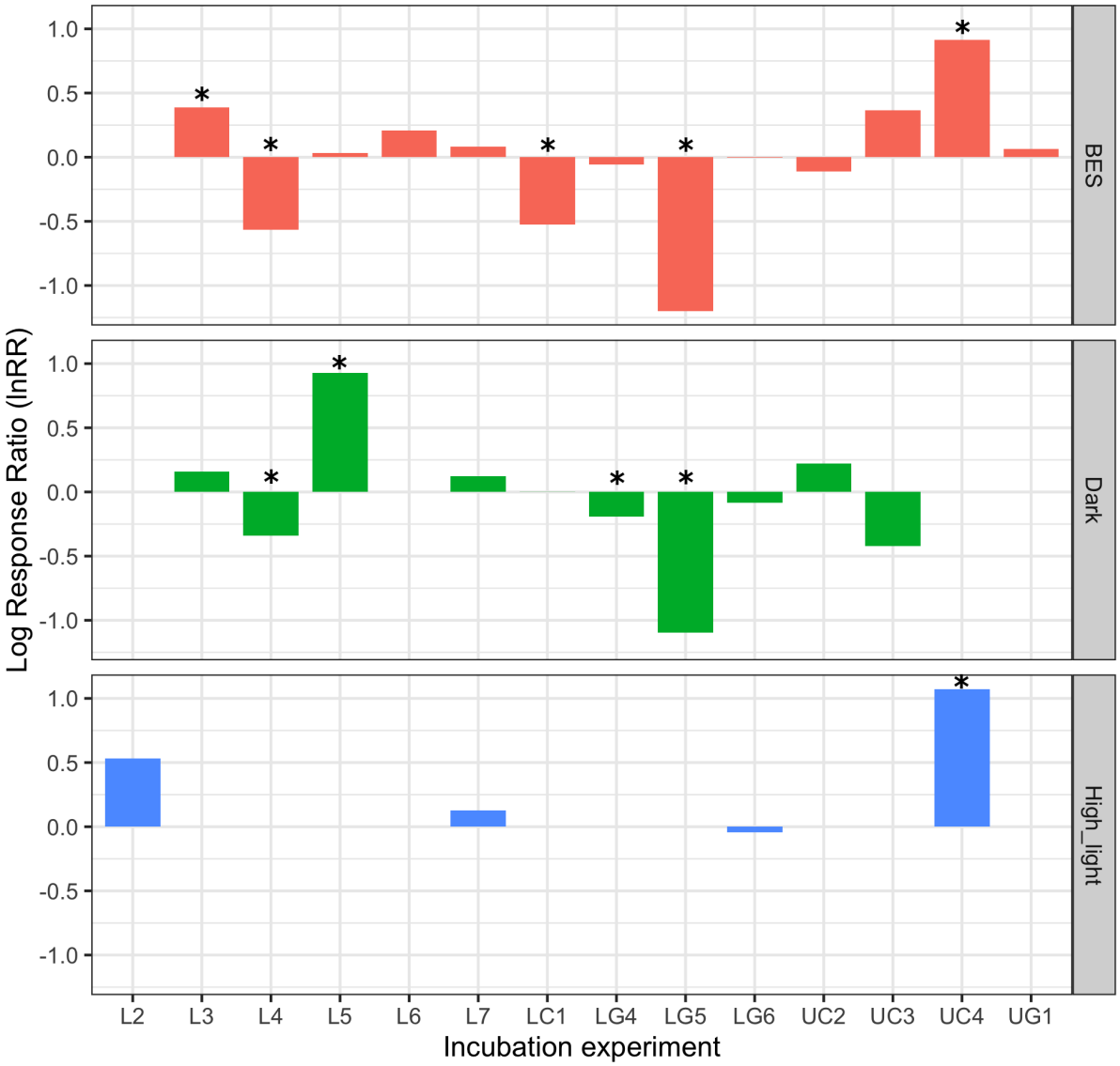

Fig. S2. Log response ratios for methane production rates in experimental treatments. Asterisks denote experimental treatments that were significantly different from the control. Experiments L3, L5, LG5 and UC3 were longer experiments and treatment effects are shown for 36, 74, 86 and 57 hours respectively (all others are shown at 24 hours).

905 **Table S1**. Percentage of *phnJ*, DPOR, and COR transcripts and genes, as well as the mean and
906 range of percent identity (ID%), for significant microbial taxa in metatranscriptomes and
907 metagenomes. Blank cells indicate that a particular group is irrelevant for that particular gene.
908

	Comamonadaceae	Cyanobacteria	*Polynucleobacter*	Other *Burkholderiales*
% of *phnJ* transcripts	20.9			
phnJ transcripts mean (and range) ID%	92.2 (69.6-100)			
% of *phnJ* genes	27.4			
phnJ genes mean (and range) ID%	84.8 (60.4-100)			
% of DPOR transcripts	30.6	6.3	5.7	2.8
DPOR transcripts mean (and range) ID%	88.8 (60.4-100)	91.5 (63.5-100)	94.5 (69.7-100)	92.1 (60.2-100)
% of DPOR genes	25.7	0.3	35.3	1.4
DPOR genes mean (and range) ID%	86.2 (60-100)	86.9 (64.4-100)	89.8 (60-100)	88.2 (60-100)
% of COR transcripts	48.7		5.8	6.8
COR transcripts mean (and range) ID%	91.5 (60-100)		94.3 (61.4-100)	93.6 (61.7-100)
% of COR genes	29.8		34.1	2.4
COR genes mean (and range) ID%	88.5 (60-100)		90.7 (60-100)	87.3 (60-100)

909
910
911

912 **Table S2.** Percent identify of 16S rRNA sequences from abundant *Comamonadaceae* ASVs to
913 those in sequenced genomes in the RefSeq Genome Database.
914

ASV	%ID	Genome
b66e24bf473f06a1fc27fa300549636c	99.7	Limnohabitans Rim47 and others, Acidovorax radicis and others
14f5d35b60a4aa29fb4630dc0531b12e	99.1	Acidovorax temperans, delafieldii and other strains
f361f2ed2d8297ddacd4e36526eb8265	100	Limnohabitans Rim11
f2fce6a8c3a54fda2ae66977fd9b45af	99	Limnohabitans Rim11 and MMS10
222b12c7663803b96339c5af33e2b3ae	100	Limnohabitans 103DPR2
9b6d5192b8dc30e78ce626298c8a0a26	99.4	Limnohabitans Rim47 and others, Acidovorax radicis and others
95dd5f1247bb97a138d1faf91e409f85	99.3	Limnohabitans 103DPR2 and JirII
62767018de03c34a4305384df06ce393	98.8	Acidovorax delafieldii, others
86832a3826a81807da70809f71eed601	99.4	Limnohabitans Rim47 and others, Acidovorax radicis and others
5efb46c72256df114e8f2b354fb44192	99.7	Limnohabitans Rim11 and MMS10
d81e17e704250a1f80e1005be449b274	99.4	Limnohabitans 103DPR2 and JirII
12e95e1ebf7046141228b71394bd745b	99.7	Limnohabitans planktonicus, Rim28, and others
02523daf5356885c7d28e05d5910acb3	100	Rhodoferax sediminis, ferrireducens, saidenbachensis, others
8f8863b1fba0419252ce1756ec2f9b46	100	Rhodoferax bucti strain GSA243-2
1b24e60fca2c1ce5d0e34cab586c4537	100	Polaromonas sp. YR568
d20e921d6be99c2d20fe3d688f878774	99.7	Rhodoferax bucti strain GSA243-2
74dace2780cac91c5a0d5598db981acc	100	Limnohabitans Rim47 and others, Acidovorax radicis and others
6f6aa478c9f6ad0d6f8b0a415706fa81	100	Limnohabitans curvus, others
317124a0271aaaea477061ada50e0cfb	99.4	Limnohabitans Rim8, others
c4143240980a12d00bf11daf4fefbd10	99.7	Limnohabitans Rim8, others
12fd09c14da54c5c7c412f7e493c4e16	100	Limnohabitans planktonicus, others
c4d004171ee776f1e529ea5dcb010508	100	Rhodoferax koreense strain DCY-110, Curvibacter sp. AEP1-3
405bafe3cfaf0d7ba859b721abc30c01	98.8	Comamonas terrigena (multiple strains)
1f796798ba249fd048e233237b86bf05	98.8	Pelomonas (multiple)

915
916

917 **Table S3.** Examples of multiple *phn* genes co-located on assembled contigs (>10,000 base pairs
918 in length) within metagenomes from the LG2 and L6 experiments.
919
920

Exp.	**Contig**	**bp**	***phnV***	***phnO***	***phnN***	***phnM***	***phnL***	***phnK***	***phnJ***	***phnI***	***phnH***	***phnG***	***phnF***	***phnE***	***phnD***	***phnC***
LG2	k141_33043	23126		1	1	1	1	1	1	1				1	1	1
LG2	k141_67057	20078			1	1	1	1	1	1	1	1				1
LG2	k141_174869	50613			1	1	1	1	1	1	1	1	1	1		
LG2	k141_61413	94539			1		1	1	1	1	1	1		1		1
LG2	k141_68876	34960			1	1	1	1	1	1	1	1	1	1		1
L6	k141_232042	14329	1						1	1	1	1				
L6	k141_58845	164079	1				1	1	1	1	1	1		1		
L6	k141_137475	51136			1		1	1	1	1	1	1			1	1

921

922 **Table S4.** List of betaproteobacterial metagenome-assembled genomes (MAGs) and links to
923 scaffolds containing COR, DPOR, and phosphonate metabolism genes on the Integrated
924 Microbial Genomes Microbiomes system.
925

MAG	Affiliation	COR gene scaffold(s)	DPOR gene scaffold(s)	Phosphonate metabolism genes scaffold(s)
1	*Rubrivivax*	Ga0136641_1000428	Ga0136641_1000214	Ga0136641_1000005 Ga0136641_1000835
5	*Limnohabitans*	Ga0136641_1000705	Ga0136641_1000769 Ga0136641_1001408	Ga0136641_1001116 Ga0136641_1001732
6	*Limnohabitans*	Ga0136641_1000147	Ga0136641_1000390 Ga0136641_1003698	Ga0136641_1000400 Ga0136641_1004149
18	*Limnohabitans*	Ga0136642_1003267		Ga0136642_1004820
20	*Polynucleobacter*	Ga0136642_1002146	Ga0136642_1003437	

926
927

928 **Table S5.** Details of experimental incubations, including: experiment number; year, month, and
929 days of experiment; whether methane production was significant and P-value; generation of 16S
930 rDNA, 16S rRNA, metatranscriptomes, and metagenomes; length of experiment; and treatments.
931 BES corresponds to the addition of 2-bromoethanesulphonate as a methanogenesis inhibitor,
932 Dark represents experiments incubated in total darkness and HL (high-light) are experiments
933 subjected to high-light intensity during the incubation.
934

Exp.	**Y**	**M**	**D**	**CH_4**	***P***	**16S rDNA**	**16S rRNA**	**Metat**	**Metag**	**Length (hr)**	**Treatments**
L1	2016	8	12-13	+	0.02	X				24	
L2	2016	9	11-12	+	0.02	X				24	HL
L3	2017	7	28-30			X				48	BES, Dark
L4	2017	8	8-10			X				48	BES, Dark
L5	2017	9	26-29	-	0.02		X			74	BES, Dark
L6	2017	11	13-15			X	X	X	X	55	BES
L7	2018	9	23-28	-	0.02		X	X		96	BES, Dark, HL
LG1	2016	8	8-9	+/-	0.02	X				24	
LG2	2016	9	9-10			X			X	24	
LG3	2016	10	7-8	+	0.02	X				24	
LG4	2017	8	24-26	+	0.02	X				48	BES, Dark
LG5	2017	10	1-4				X	X		86	BES, Dark
LG6	2018	9	10-14				X	X		96	BES, Dark, HL
UC1	2016	8	10-11	+	0.02	X				24	
UC2	2017	8	10-12							48	BES, Dark
UC3	2017	10	8-11	+/-	0.006		X			57	BES, Dark
UC4	2018	10	8-12				X	X		96	BES, Dark, HL
LC1	2017	08	26-28	-	0.02					48	BES, Dark
UG1	2017	08	12-14							48	BES

935
936
937

SI References

1. M. Yao, C. Henny, J. A. Maresca, Freshwater Bacteria Release Methane as a By-Product of Phosphorus Acquisition. *Appl Env. Microbiol* **82**, 6994–7003 (2016).

2. Q. Wang, J. E. Dore, T. R. McDermott, Methylphosphonate metabolism by Pseudomonas sp. populations contributes to the methane oversaturation paradox in an oxic freshwater lake. *Environ. Microbiol.* **19**, 2366–2378 (2017).

3. D. M. Karl, *et al.*, Aerobic production of methane in the sea. *Nat. Geosci.* **1**, 473–478 (2008).

4. H.-P. Grossart, K. Frindte, C. Dziallas, W. Eckert, K. W. Tang, Microbial methane production in oxygenated water column of an oligotrophic lake. *Proc. Natl. Acad. Sci.* **108**, 19657–19661 (2011).